Screening of SNP in association with the susceptibility to HCV-DCM in seven candidate genes

To identify the susceptibility gene, we examined SNPs in each of the candidate genes and compared their individual as well as their combined (haplotype) frequencies between the HCV-DCM patients and control individuals (Table 2). Of 16 *HLA-B* and 9 *HLA-Cw* alleles assigned by SBT method in HCV-DCM patients, *HLA-B*0702* (OR = 3.96, $P = 0.022$, $Pc = 0.356$) and *HLA-Cw*0702* (OR = 3.00, $P = 0.019$, $Pc = 0.192$) showed marginally significant associations with HCV-DCM. Additionally, of the seven non-*HLA* genes, we analyzed five genes, *TNF, LTA, NFKBIL1, ATP6V1G2,* and *BAT1,* in the SNP study and found three SNPs strongly associated with HCV-DCM; a T insertion at the position −421 of the *NFKBIL1* promoter (*NFKBIL1p*−421insT*) (OR = 4.25, $P = 0.003$, $Pc = 0.006$), an A to T substitution at the position +760 of the *ATP6V1G2* (*ATP6V1G2*+760T*) (OR = 4.25, $P = 0.003$, $Pc = 0.006$), and a fifth polymorphic haplotype (*BAT1p*05*) of the *BAT1* promoter (OR = 4.25, $P = 0.003$, $Pc = 0.006$) (Table 2). The *NFKBIL1p*−421insT* and *ATP6V1G2*+760T* are characteristic polymorphisms of the *NFKBIL1p*02* and *ATP6V1G2*3* alleles, respectively, which exhibited equivalent associations with HCV-DCM (Table 2). In contrast, neither *TNF* nor *LTA* polymorphisms showed significant association with HCV-DCM (data not shown).

Pairwise LD mapping around the candidate region in the Japanese population

Interestingly, the combination of the non-*HLA* gene alleles, consisting of *NFKBIL1p*02, ATP6V1G2*3,* and *BAT1p*05,* which were

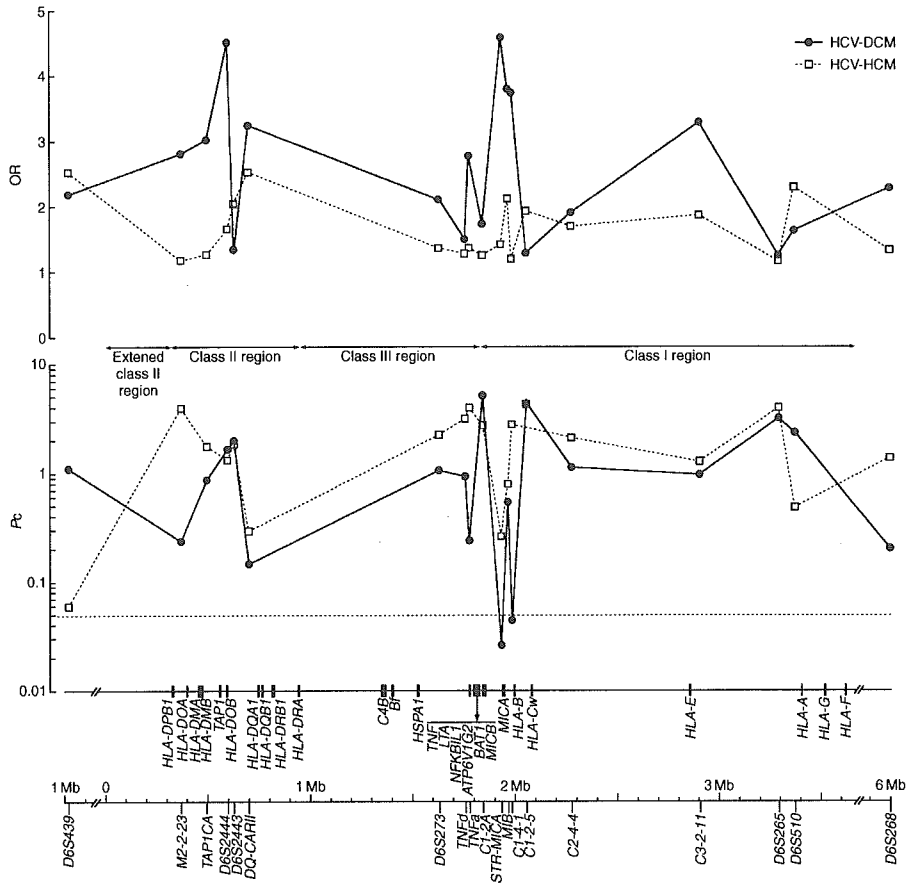

Fig. 1. **The susceptibility gene mapping for hepatitis C virus-associated dilated cardiomyopathy (HCV-DCM) and HCV-hypertrophic cardiomyopathy (HCV-HCM) with microsatellite markers throughout the human major histocompatibility complex genomic region.** Corrected *P* (*Pc*) value with logarithmic scale and odds ratio (*y*-axis) were plotted against physical location of the microsatellite markers on chromosome 6p21.3 (*x*-axis), their distance (in kb) in order from centromere to telomere. The dotted horizontal line shows the threshold for 5% significance after correcting for multiple testing.

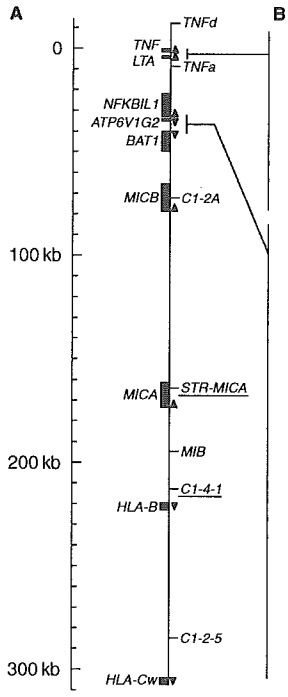

B

TNF promoter

Haplotype	−1031	−963	−857	−308	−238	HF
A	T	C	C	G	G	0.628
B	C	A	C	G	G	0.164
C	C	C	C	G	A	0.015
D	T	C	T	G	G	0.019
E	T	C	C	A	G	0.004

LTA

Haplotype	+80	+252	HF
1	A	A	0.453
2	C	A	0.193
3	C	G	0.354

NFKBIL1 promoter

Haplotype	−421	−325	−263	63	HF
01	D	C	A	T	0.380
02	I	C	A	T	0.091
03	D	C	G	T	0.182
04	D	G	A	A	0.036
05	D	C	A	A	0.310

ATP6V1G2

Haplotype	+760	+1222	HF
1	A	C	0.876
2	A	T	0.033
3	T	C	0.091

BAT1 promoter

Haplotype	−1382	−1178	−1176	−1167	−1101	−1058	−573	−348	−210	−22	HF
01	T	C	G	T	G	I	I	C	C	C	0.351
02	T	G	T	C	G	I	I	C	C	G	0.208
03	T	T	T	T	A	D	I	T	C	G	0.171
04	T	G	T	T	G	I	I	C	A	G	0.139
05	T	G	T	T	A	I	I	T	C	G	0.091
06	G	G	T	T	G	I	I	C	A	G	0.022
07	T	C	G	T	G	I	D	C	C	C	0.014

Fig. 2. **Candidate gene mapping in a susceptible 300-kb interval to hepatitis C virus-associated dilated cardiomyopathy (HCV-DCM).** (A) The physical map of candidate genes and genetic markers in the 300-kb interval. Microsatellite markers showing strong association with HCV-DCM in the microsatellite analyses were underlined. Arrow heads indicated the transcriptional direction of candidate genes. (B) Haplotype structures at the candidate gene loci. Haplotype frequencies (HF) were estimated by EM algorithms in the R package 'haplo.stats' (http://www.r-project.org/). Designations refer to the nucleotide position to transcriptional start site. Allelic sequences were defined by the same forward sequence as transcriptional direction in the genes. The I and D carried at *NFKBIL1p*−421*, *BAT1p*−1058*, and *BAT1p*−573* indicate the insertion and the deletion (indel), respectively. The indels carry allelic forms as follows (in order from 5′ to 3′): T/− at the *NFKBIL1p*−421*, AGG/− at the *BAT1p*−1058*, and CATCAGCTACCTCGGA/− at the *BAT1p*−573*.

significantly associated with HCV-DCM were tightly linked as a non-HLA haplotype block in a one-to-one correspondence in both patients and controls. This linkage was expected to result from a characteristic LD relationship in Japanese. We, therefore, evaluated the LD indexes for the specific LD block using other 15 polymorphic markers around the central MHC genomic region in the Japanese controls (Table 3). The pairwise LD mapping confirmed that these three alleles are in complete LD with each other, showing LD index being 1.0 for D' and 1.0 for r^2. In addition, *HLA-B*0702* was in strong LD not only with *HLA-Cw*0702* ($D' = 1.0$, $r^2 = 0.43$) but also with this non-HLA haplotype block ($D' = 1.0$, $r^2 = 0.59$).

The risk evaluation of the patient-shared block in HCV-DCM

We subsequently evaluated the non-HLA haplotype block as the main risk marker for HCV-DCM (Table 4). The analysis showed that a higher risk was conferred by *Hap A* (OR = 6.75, $P = 0.0003$, $Pc = 0.0081$) from the MHC class III – class I boundary region than by *Hap B* (OR = 3.96, $P = 0.02$, $Pc = 0.40$) from the MHC class I region. This strongly suggests that the disease susceptibility to HCV-DCM is controlled mainly by the non-*HLA* genes in the MHC class III – class I boundary region rather than by the classical *HLA* class I genes. The strong LD between *TNF* gene cluster and *NFKBIL1-BAT1* block also prompted us to examine a synergistic risk for HCV-DCM between *TNFp*A-LTA*1* and *NFKBIL1p*02-ATP6V1G2*3-BAT1*05-C1-2A*242-STR-MICA*183* by two-locus-analysis method of Svejgaard and Ryder (31). However, no synergistic risk between the haplotypes was found (data not shown). In light of location of the polymorphic markers composing of *Hap A*, the primary susceptibility locus could be narrowed down to approximately 133-kb interval between the *NFKBIL1* and *MICA* genes.

Discussion

It is well established that the *HLA* genes in the MHC have an important role in the regulation of immune response to acute and persistent HCV infection. The aim of this study was to investigate whether the non-*HLA* genes and *HLA* genes in the MHC might be associated with the susceptibility to HCV-DCM and/or HCV-HCM. Our MHC region-wide association study mapped the HCV-DCM susceptibility locus to the region spanning from *NFKBIL1* to *MICA* within the MHC class III – class I boundary region. In addition, the polymorphisms located around this boundary region were in LD with the classical *HLA-B* and *HLA-Cw* class I gene alleles. These observations suggest that the susceptibility to HCV-DCM may

Associations of candidate gene polymorphisms relevant to hepatitis C virus-associated dilated cardiomyopathy susceptibility within the central major histocompatibility complex region

	Genotype[a]									
	Cases (n = 21)			Controls (n = 120)			Carriers versus non-carriers			
Marker	++	+−	−−	++	+−	−−	OR	95% CI	P	Pc
Allele										
*NFKBIL1p*02*	1	8	12	0	18	102	4.25	1.57 - 11.54	0.003	0.014
*ATP6V1G2*3*	1	8	12	0	18	102	4.25	1.57 - 11.54	0.003	0.008
*BAT1p*05*	1	8	12	0	18	102	4.25	1.57 - 11.54	0.003	0.014
*HLA-B*0702*	0	6	15	0	11	109	3.96	1.28 - 12.29	0.022	0.356
*HLA-Cw*0702*	1	8	12	0	24	96	3.00	1.13 - 7.94	0.019	0.192
Polymorphism										
−421insT of *NFKBIL1*	1	8	12	0	18	102	4.25	1.57 - 11.54	0.003	0.005
+760T of ATP6V1G2	1	8	12	0	18	102	4.25	1.57 - 11.54	0.003	0.005

[a]++, homozygous carrier with the targeted polymorphisms; +−, heterozygous; −−, non-carrier

Table 2

be controlled by the non-*HLA* genes in LD with the *HLA* class I gene alleles rather than the *HLA* genes.

The mapped candidate susceptibility gene locus for HCV-DCM within the MHC class III – class I boundary region overlaps the susceptibility/resistance loci for some autoimmune diseases, such as rheumatoid arthritis (14) and insulin-dependent diabetes mellitus (32). Some candidate genes within the class III – class I boundary region that control the susceptibility to HCV-DCM encode molecules that are probably involved in immunity and inflammation. For example, *NFKBIL1* gene encodes a I-kappa-B-like molecule (33), which localizes within nuclear speckles (34). The product of *ATP6V1G2* gene responds to IL-1 as a subunit of vacuolar ATPase H^+ pump and modulates macrophage effector functions (35, 36). The role of the BAT1 proteins is less well defined, but they may act as negative regulators of an inflammatory cytokine (37) and effect cell proliferation in various human tissues including the heart (38). *MICA* and *MICB* genes exhibit a restricted expression pattern on cell in stress like those after viral infection (39–41) and may play a role in HCV infectious status as ligand of NKG2D (42, 43). These reported functions for the five non-*HLA* genes around the MHC class III – class I boundary region are helpful in explaining the genetic background of HCV-DCM, but cellular studies are clearly needed to determine the direct effect of HCV infection on the activity and the role of *NFKBIL1*, *ATP6V1G2*, *BAT1*, *MICB*, and *MICA* genes in the heart.

The candidate susceptibility locus identified in this study contained several functional SNPs, which might regulate transcriptional efficiency of the candidate genes. One such interesting SNPs is *NFKBIL1p*−62T/A* that lies within an E-box-binding motif (CANNTG) for transcriptional factors, E47 and USF1 (44). Second, the sequence spanning *BAT1p*−22G/C* (GCAGAT) and *BAT1p*−348C/T* (CCAT) is known to affect the *BAT1* expression via direct interaction with their transcriptional factors, Oct1 and YY1, respectively (45). These multiple functional polymorphisms may therefore combine functionally to increase the risk of DCM under the HCV infection. There were, however, still many ethnically characteristic and/or functionally unknown promoter polymorphisms other than the aforementioned SNPs. A transgenic mouse study revealed that the HCV-core protein is directly involved in the development of cardiomyopathy (46). The extent to which such polymorphisms influence the pathogenesis of HCV-DCM is a subject of further study.

Despite the same viral etiology, HCV involvement in cardiomyopathy can result in two distinct clinical outcomes, HCV-DCM and HCV-HCM, and a difference in the association with the MHC was revealed in this study. Whereas the microsatellite markers displayed a significant association of a particular MHC subregion with HCV-DCM, there was no significant association between the MHC and HCV-HCM. The HLA haplotypic markers in association with HCV-DCM are in strong LD with *B*0702-Cw*0702*, which are in LD with *DRB1*0101-DQB1*0501* in Japanese (47). However, these *HLA* alleles were not associated with HCV-associated liver diseases (22). In addition, a tendency toward severe HCV-infection status in Spanish whites was associated with *HLA-DR3-MICA-A4-HLA-B*18* (48); however, HCV-DCM patients in the present study showed

Tissue Antigens 2005: 66: 200–208

Pairwise linkage disequilibrium (LD) analysis of hepatitis C virus-associated dilated cardiomyopathy susceptibility loci for 120 Japanese individuals

		r^2														
Locus		*TNFd*130*	*TNFp*A*	*LTA*1*	*TNFa*115*	*NFKBIL1p*02*	*ATP6V1G2*3*	*BAT1p*05*	*C1-2A*242*	*STR-MICA*183*	*MIB*336*	*C1-4–1*225*	*HLA-B*0702*	*C1-2-5*200*	*HLA-Cw* 0702*	*C2-4-4* 231*
	*TNFd*130*	–	0.19	0.23	0.30	0.14	0.14	0.14	0.52	0.01	0.04	0.07	0.09	0.01	0.06	0.03
	*TNFp*A*	0.46	–	0.00	0.04	0.05	0.05	0.05	0.15	0.01	0.06	0.01	0.03	0.04	0.00	0.01
	*LTA*1*	0.59	0.06	–	0.16	0.10	0.10	0.10	0.31	0.01	0.01	0.05	0.06	0.01	0.05	0.01
	*TNFa*115*	**0.95**	0.35	**0.85**	–	0.32	0.32	0.32	0.35	0.05	0.13	0.08	0.25	0.04	0.12	0.06
	*NFKBIL1p*02*	**1.00**	**1.00**	**1.00**	**0.86**	–	**1.00**	**1.00**	0.16	0.24	0.26	0.34	**0.59**	0.14	0.33	0.05
	*ATP6V1G2*3*	**1.00**	**1.00**	**1.00**	**0.86**	**1.00**	–	**1.00**	0.16	0.24	0.26	0.34	**0.59**	0.14	0.33	0.05
	*BAT1p*05*	**1.00**	**1.00**	**1.00**	**0.86**	**1.00**	**1.00**	–	0.16	0.24	0.26	0.34	**0.59**	0.14	0.33	0.05
D'	*C1-2A*242*	**0.85**	0.47	0.80	**0.87**	**0.90**	**0.90**	**0.90**	–	0.04	0.04	0.07	0.12	0.04	0.06	0.03
	*STR-MICA*183*	0.23	0.35	0.20	0.26	0.66	0.66	0.66	0.34	–	0.18	0.16	0.32	0.04	0.14	0.09
	*MIB*336*	0.46	**1.00**	0.26	0.50	0.55	0.55	0.55	0.39	0.53	–	0.34	**0.50**	0.10	0.21	0.01
	*C1-4-1*225*	0.66	0.45	0.69	0.40	0.62	0.62	0.62	0.54	0.50	0.60	–	**0.53**	0.08	**0.64**	0.06
	*HLA-B*0702*	**1.00**	**1.00**	**1.00**	**1.00**	**1.00**	**1.00**	**1.00**	**1.00**	**1.00**	**1.00**	**1.00**	–	0.23	**0.43**	0.05
	*C1-2-5*200*	0.18	0.55	0.16	0.21	0.61	0.61	0.61	0.28	0.25	0.46	0.43	**1.00**	–	0.06	0.12
	*HLA-Cw*0702*	0.55	0.10	0.61	0.46	0.67	0.67	0.67	0.46	0.44	0.49	**0.89**	**1.00**	0.34	–	0.11
	*C2-4-4*231*	0.22	0.11	0.08	0.57	0.79	0.79	0.79	0.30	0.79	0.40	**0.81**	**1.00**	0.77	**1.00**	–

Each polymorphic marker was positioned in order from major histocompatibility complex class III to class I subregion. The degree of LD is shown as the LD index of Lewontin correlation (D') in the lower left triangle and Pearson correlation (r^2) in the upper right triangle. Bold number indicates the strong LD: $D' > 0.8$, $r^2 > 0.4$. The solid LD block of genes from the class III region with the highest LD are boxed.

Table 3

Haplotype structures composed of significantly increased markers and single nucleotide polymorphisms (SNPs) in HCV-associated dilated cardiomyopathy

	Diplotype[a]									
	Cases (n = 21)			Control (n = 120)			Carriers versus non-carriers			
Haplotype	++	+−	−−	++	+−	−−	OR	95% CI	P	P_C
Hap A (MHC class III – class I boundary region side)										
*NFKBIL1p*02-ATP6V1G2*3-BAT1p*05-STR-MICA*183*	1	8	12	0	13	107	6.17	2.19 – 17.45	0.0005	0.0131
Hap B (MHC class I region)										
*B*0702-Cw*0702*	0	6	15	0	11	109	3.96	1.28 – 12.29	0.02	0.40

[a]++, homozygous carrier with the targeted haplotypes; +−, heterozygous; −−, non-carrier

Table 4

a different association with the *DRB1*0101-STR-MICA*183* (also known as *MICA-A5.1)-B*0702* haplotype. These haplotypic differences may indirectly reflect the genetic diversity among non-*HLA* genes that define each HLA haplotypes. Thus, these observations support the view that distinct genetic factors can affect the clinical outcome by regulating pathogenic pathway after the viral infection.

In summary, our susceptibility gene mapping showed that the non-*HLA* gene block consisting of the *NFKBIL, ATP6V1G2, BAT1, MICB*, and *MICA* genes within the MHC class III – class I boundary region was strongly associated with the susceptibility to HCV-DCM, whereas there was no significant association between the MHC genomic region and HCV-HCM. Through the disparity in the disease-associated HLA markers, we hypothesize that HCV-DCM and HCV-HCM have at least two distinct pathogenic mechanisms in relation to the MHC-meditated immune response, although the patients that developed DCM/HCM with HCV infection consisted of a small number of cases. Because the conclusions were based on the analysis of small number of patients, other independent studies with larger number of patients will be required. Nevertheless, our findings may provide an important clue as to the underlying cause of HCV-DCM in terms of immunogenetics. Because of tight LD among non-*HLA* alleles within the candidate genes, we could not identify specific susceptibility gene for HCV-DCM. Therefore, analysis of central MHC region in other Asian ethnic groups with HCV-DCM may contribute to a delineation of primary locus to the HCV-DCM susceptibility. Genome-wide microsatellite association studies in a much larger sample of infected patients will be also required to comprehensively understand their genetic background and the effect of genetic diversity on the outcome of HCV-associated cardiomyopathies.

References

1. Higuchi M, Tanaka E, Kiyosawa K. Epidemiology and clinical aspects on hepatitis C. *Jpn J Infect Dis* 2002: **55**: 69–77.
2. Mayo MJ. Extrahepatic manifestations of hepatitis C infection. *Am J Med Sci* 2003: **325**: 135–48.
3. Yan FM, Chen AS, Hao F et al. Hepatitis C virus may infect extrahepatic tissues in patients with hepatitis C. *World J Gastroenterol* 2000: **6**: 805–11.
4. Matsumori A, Matoba Y, Sasayama S. Dilated cardiomyopathy associated with hepatitis C virus infection. *Circulation* 1995: **92**: 2519–25.
5. Matsumori A, Matoba Y, Nishio R et al. Detection of hepatitis C virus RNA from the heart of patients with hypertrophic cardiomyopathy. *Biochem Biophys Res Commun* 1996: **222**: 678–82.
6. Takeda A, Sakata A, Takeda N. Detection of hepatitis C virus RNA in the hearts of patients with hepatogenic cardiomyopathy. *Mol Cell Biochem* 1999: **195**: 257–61.
7. Teragaki M, Nishiguchi S, Takeuchi K et al. Prevalence of hepatitis C virus infection among patients with hypertrophic cardiomyopathy. *Heart Vessels* 2003: **18**: 167–70.
8. Matsumori A, Ohashi N, Hasegawa K et al. Hepatitis C virus infection and heart diseases: a multicenter study in Japan. *Jpn Circ J* 1998: **62**: 389–91.
9. Cooke GS, Hill AV. Genetics of susceptibility to human infectious disease. *Nat Rev Genet* 2001: **2**: 967–77.
10. Shiina T, Inoko H, Kulski JK. An update of the HLA genomic region, locus information and disease associations: 2004. *Tissue Antigens* 2004: **64**: 631–49.
11. Marsh SG, Albert ED, Bodmer WF et al. Nomenclature for factors of the HLA system, 2002. *Hum Immunol* 2002: **63**: 1213–68.
12. Robinson J, Waller MJ, Parham P et al. IMGT/HLA and IMGT/MHC: sequence databases for the study of the major histocompatibility complex. *Nucl Acids Res* 2003: **31**: 311–4.
13. Mungall AJ, Palmer SA, Sims SK et al. The DNA sequence and analysis of human chromosome 6. *Nature* 2003: **425**: 805–11.

14. Okamoto K, Makino S, Yoshikawa Y et al. Identification of I kappa BL as the second major histocompatibility complex-linked susceptibility locus for rheumatoid arthritis. *Am J Hum Genet* 2003: **72**: 303–12.
15. Ozaki K, Ohnishi Y, Iida A et al. Functional SNPs in the lymphotoxin-alpha gene that associated with susceptibility to myocardial infraction. *Nat Genet* 2002: **32**: 650–4.
16. Knight JC, Udalova I, Hill AV et al. A polymorphism that affects OCT-1 binding to the TNF promoter region is associated with severe malaria. *Nat Genet* 1999: **22**: 145–50.
17. Mira J. Association of TNF2, a TNF-alpha promoter polymorphism, with septic shock susceptibility and mortality: a multicenter study. *JAMA* 1999: **282**: 561–8.
18. Burch GH, Gong Y, Liu W et al. Tenascin-X deficiency is associated with Ehlers-Danos syndrome. *Nat Genet* 1997: **17**: 104–8.
19. Ahmad T, Neville M, Marshall SE et al. Haplotype-specific linkage disequilibrium patterns define the genetic topography of the human MHC. *Hum Mol Genet* 2003: **12**: 647–56.
20. Walsh EC, Mather KA, Schaffner SF et al. An integrated haplotype map of the human major histocompatibility complex. *Am J Hum Genet* 2003: **73**: 580–90.
21. Stenzel A, Lu T, Koch WA et al. Patterns of linkage disequilibrium in the MHC region on human chromosome 6p. *Hum Genet* 2004: **114**: 377–85.
22. Kuzushita N, Hayashi N, Moribe T et al. Influence of HLA haplotypes on the clinical courses of individuals infected with hepatitis C virus. *Hepatology* 1998: **27**: 240–4.
23. Research Committee on Idiopathic Cardiomyopathy, the Ministry of the Health and Welfare, Japan. Guidelines for the diagnosis of idiopathic cardiomyopathy. In: *Annual Report of the Research Committee on Idiopathic Cardiomyopathy, the Ministry of the Health and Welfare, Japan*, 1985: 13–5 (in Japanese).
24. The WHO, /ISFC task force on the definition and classification of cardiomyopathies. Report of the WHO/ISFC task force on the definition and classification of cardiomyopathies. *Br Heart J* 1980: **44**: 672–3.
25. Foissac A, Salhi M, Cambon-Thomsen A. Microsatellites in the HLA region: 1999 update. *Tissue Antigens* 2000: **55**: 477–509.
26. Cullen M, Malasky M, Harding A, Carrington M. High-density map of short tandem repeats across the human major histocompatibility complex. *Immunogenetics* 2003: **54**: 900–10.
27. Higuchi T, Seki N, Kamizono S et al. Polymorphism of the 5′-flanking region of the human tumor necrosis factor (TNF)-alpha gene in Japanese. *Tissue Antigens* 1998: **51**: 605–12.
28. Allcock RJ, Baluchova K, Cheong KY, Price P. Haplotypic single nucleotide polymorphisms in the central MHC gene IKBL, a potential regulator of NF-kappaB function. *Immunogenetics* 2001: **52**: 289–93.
29. Wong AM, Allcock RJ, Cheong KY, Christiansen FT, Price P. Alleles of the proximal promoter of BAT1, a putative anti-inflammatory gene adjacent to the TNF cluster, reduce transcription on a disease-associated MHC haplotype. *Genes Cells* 2003: **8**: 403–12.
30. Knight JC, Keating BJ, Kwiatkowski DP. Allele-specific repression of lymphotoxin-alpha by activated B cell factor-1. *Nat Genet* 2004: **36**: 394–9.
31. Svejgaard A, Ryder LP. HLA and disease associations: detecting the strongest association. *Tissue Antigens* 1994: **43**: 18–27.
32. Yamashita T, Hamaguchi K, Kusuda Y . IKBL promoter polymorphism is strongly associated with resistance to type 1 diabetes in Japanese. *Tissue Antigens* 2004: **63**: 223–30.
33. Albertella MR, Campbell RD. Characterization of a novel gene in the human major histocompatibility complex that encodes a potential new member of the I kappa B family of proteins. *Hum Mol Genet* 1994: **3**: 793–9.
34. Semple JI, Brown SE, Sanderson CM et al. A distinct bipartite motif is required for the localization of inhibitatory kappaB-like (IkappaBL) protein to nuclear speckles. *Biochem J* 2002: **361**: 489–96.
35. Conboy IM, Manoli D, Mhaiskar V, Jones PP. Calcineurin and vacuolar-type H+-ATPase modulate macrophage effector functions. *Proc Natl Acad Sci USA* 1999: **96**: 6324–9.
36. Brisseau GF, Grinstein S, Hackam DJ et al. Interleukin-1 increases vacuolar-type H+-ATPase activity in murine peritoneal macrophages. *J Biol Chem* 1996: **27**: 2005–11.
37. Allcock RJ, Williams JH, Price P. The central MHC gene, BAT1, may encode a protein that down-regulates cytokine production. *Genes Cells* 2001: **6**: 487–94.
38. Leaw CL, Ren EC, Choong ML. Hcc-1 is a novel component of the nuclear matrix with growth inhibitory function. *Cell Mol Life Sci* 2004: **61**: 2264–73.
39. Groh V, Bahram S, Bauer S et al. Cell stress-regulated human major histocompatibility complex class I gene expressed in gastrointestinal epithelium. *Proc Natl Acad Sci USA* 1996: **93**: 12445–50.
40. Zwirner NW, Dole K, Stastny P. Differential surface expression of MICA by endothelial cells, fibroblasts, keratinocytes, and monocytes. *Hum Immunol* 1999: **60**: 323–30.
41. Molinero LL, Fuertes MB, Girart MV et al. NF-kappa B regulates expression of the MHC class I-related chain A gene in activated T lymphocytes. *J Immunol* 2004: **173**: 5583–90.
42. Karacki PS, Gao X, Thio CL et al. MICA and recovery from hepatitis C virus and hepatitis B virus infections. *Genes Immun* 2004: **5**: 261–6.
43. Jinushi M, Takehara T, Tatsumi T et al. Autocrine/paracrine IL-15 that is required for type I IFN-meditated dendritic cell expression of MHC class I-related chain A and B is impaired in hepatitis C virus infection. *J Immunol* 2003: **171**: 5423–9.
44. Boodhoo A, Wong AM, Williamson D et al. A promoter polymorphism in the central MHC gene, IKBL, influences the binding of transcription factors USF1 and E47 on disease-associated haplotypes. *Gene Exp* 2004: **12**: 1–11.
45. Price P, Wong AM, Williamson D et al. Polymorphisms at positions -22 and – 348 in the promoter of the BAT1 gene affect transcription and the binding of nuclear factors. *Hum Mol Genet* 2004: **13**: 967–74.
46. Omura T, Yoshiyama M, Hayashi T et al. Core protein hepatitis C virus induces cardiomyopathy *Circ Res* 2005: **96**: 148–50.
47. Saito S, Ota S, Yamada E, Inoko H, Ota M. Allele frequencies and haplotypic associations defined by allelic DNA typing at HLA class I and class II loci in the Japanese population. *Tissue Antigens* 2000: **56**: 522–9.
48. López-Vázquez A, Rodrigo L, Miña-Blanco A et al. Extended human leukocyte antigen haplotype EH18.1 influences progression to hepatocellular carcinoma in patients with hepatitis C virus infection. *J Infect Dis* 2004: **189**: 957–63.

Genotypes at chromosome 22q12-13 are associated with HIV-1-exposed but uninfected status in Italians

Yasuyoshi Kanari[a], Mario Clerici[b], Hiroyuki Abe[a], Hiroyuki Kawabata[a], Daria Trabattoni[b], Sergio Lo Caputo[c], Francesco Mazzotta[c], Hironori Fujisawa[d], Atsuko Niwa[a], Chiaki Ishihara[e], Yumiko A. Takei[f] and Masaaki Miyazawa[a]

Objective: Despite multiple and repeated exposures to HIV-1, some individuals possess no detectable HIV genome and show T-cell memory responses to the viral antigens. HIV-1-reactive mucosal IgA detected in such uninfected individuals suggests their possible immune resistance against HIV. We tested if the above HIV-1-exposed but uninfected status was associated with genetic markers other than a homozygous deletion of the *CCR5* gene.

Methods: Based on our mapping in chromosome 15 of a gene controlling the production of neutralizing antibodies in a mouse retrovirus infection, we genotyped 42 HIV-1-exposed but uninfected Italians at polymorphic loci in the syntenic segment of human chromosome 22, and compared them with 49 HIV-1-infected and 47 uninfected healthy control individuals by a closed testing procedure.

Results: A significant association was found between chromosome 22q12-13 genotypes and a putative dominant locus conferring anti-HIV-1 immune responses in the exposed but uninfected individuals. Distributions of linkage disequilibrium across chromosome 22 also differed between the exposed but uninfected and two other phenotypic groups.

Conclusions: The data indicated the presence of a new genetic factor associated with the HIV-1-exposed but uninfected status.

AIDS 2005, **19**:1015–1024

Keywords: HIV-1, exposed seronegatives, genetic background, chromosome 22, neutralizing antibody, synteny, association study

Introduction

The absence of clinical progression in some HIV-1-infected individuals and the lack of a detectable HIV-1 genome despite multiple and repeated exposures to this virus in some groups of people are noteworthy phenomena when considering the development of preventative and therapeutic means to HIV infection [1–3]. There are individuals who show strong HIV-1 antigen-specific T-lymphocyte responses and HIV-1-reactive mucosal IgA production despite the absence of detectable plasma HIV-1 RNA and HIV-1 cDNA from peripheral blood mononuclear cells (PBMC) [4–6]. HIV-1-neutralizing activity exerted by the IgA isolated from some HIV-1-exposed but uninfected individuals (EUI) [7–9] has suggested a possible contribution of the

From the [a]Department of Immunology, Kinki University School of Medicine, Osaka-Sayama, Osaka, Japan, the [b]Department of Immunology, DISP LITA Vialba, Milano University Medical School, Milano, Italy, the [c]Infectious Diseases Unit, Ospedale Santa Maria Annunziata, Firenze, Italy, the [d]The Institute of Statistical Mathematics, Tokyo, Japan, the [e]Department of Laboratory Animal Sciences, School of Veterinary Medicine, Rakuno Gakuen University, Ebetsu, Japan, and the [f]Department of Pathology, Tohoku University School of Medicine, Sendai, Japan.

Correspondence to M. Miyazawa, Department of Immunology, Kinki University School of Medicine, 377-2 Ohno-Higashi, Osaka-Sayama, Osaka 589-8511, Japan.

E-mail: masaaki@med.kindai.ac.jp.

Received: 26 August 2004; revised: 27 January 2005; accepted: 2 February 2005.

host immune responses to the resistance against HIV infection. However, genetic factors that may influence the observed T-cell priming and the production of anti-HIV-1 IgA without the establishment of HIV replication are currently unknown.

Host genetic factors influencing viral entry and replication and antiviral immune responses have been extensively studied in mouse models of retroviral infections, among which the best analyzed is Friend mouse leukemia virus complex (FV) [10–13]. Host gene loci that control the entry and replication of FV in the target cells have been identified [14–17]. In addition, MHC class II loci directly restrict the T-helper cell recognition of the viral antigens [18–20], while a class I locus influences the production of cytokines from virus-specific T cells [21]. Another locus that has been mapped to chromosome 15 strongly influences the persistence of viremia after FV infection [12,22–25]. However, the possible relationship between the above persistence of viremia and production of virus-neutralizing antibodies has not been directly examined. Here we have performed linkage analyses on a mouse locus that influences the production of virus-neutralizing antibodies upon FV infection. An extension of this mouse study unexpectedly led us to find human chromosomal markers that are associated with the presence of HIV-1-reactive immune responses in HIV-uninfected individuals.

Methods

Mice, virus, and assays for neutralizing antibodies

B10.A and A/WySn mice were purchased from Japan SLC, Inc., Hamamatsu, Japan and The Jackson Laboratory, Bar Harbor, Maine, USA, respectively. The F_1 crosses and backcross mice were bred and maintained at Rakuno Gakuen University and Kinki University School of Medicine under specific pathogen-free conditions. The following experiments were approved by and performed under guidelines of each university. FV was prepared and inoculated as described [18,20–27]. FV-neutralizing antibodies were titered by immunoenzymatically visualizing foci of virus infection as described [20,26,27].

Analyses of simple sequence length polymorphisms (SSLP) and linkage mapping in mice

Genomic DNA was prepared from the tail tip of each mouse using DNeasy Tissue Kit (QIAGEN GmbH, Hilden, Germany). A pair of oligonucleotide primers for each microsatellite locus was designed based on the sequence information listed in the Genetic and Physical Maps of the Mouse Genome site (http://www-genome.wi.mit.edu/cgi-bin/mouse/) and ordered from QIAGEN GmbH. Fifty nanogrmas of each template DNA was subjected to 35 cycles of PCR amplification using a recombinant *Taq* polymerase (Invitrogen Life Technologies, Carlsbad, California, USA). PCR products were separated by electrophoresis in 4% agarose gel and visualized by ethidium bromide staining. Correlation between genotypes at each examined locus and the presence or absence of virus-neutralizing antibodies was analyzed by Pearson's χ^2 test. Map orders of the chromosomal loci and log-of-the-odds (LOD) scores were determined by multipoint analyses using MAPMAKER/EXP version 3.0b (The Whitehead Institute, Massachusetts, USA).

EUI and HIV-1-infected individuals

Forty-two heterosexual couples discordant for HIV-1 serostatus were enrolled. The female partner was HIV-1-infected in 32 couples, whereas the male partner was HIV-1-infected in the remaining 10 couples. The diagnosis of HIV-1 infection was made based on the detection of plasma HIV-1 RNA before the initiation of antiretroviral drug treatment and significant titers of serum anti-HIV-1 IgG antibody as described in the following section. The inclusion criteria for the EUI group were a history of multiple unprotected sexual episodes for >4 years with an average of eight reported unprotected sexual contacts per year (range 5 to >40) at the time of inclusion, and at least three episodes of at-risk intercourses within 4 months prior to the study point. Forty-two of the 49 HIV-1-infected individuals studied here are the steady and reportedly monogamous partners of the above EUI individuals. In all the infected individuals the diagnosis of HIV-1 infection was made during their chronic phase, and thus unprotected sexual intercourses had been initiated long before their diagnosis. Mean CD4 cell count of the infected partners at the time of this study was 370×10^6/l (range 36×10^6–850×10^6/l). Seven additional age- and sex-matched HIV-1-infected individuals were added to the study, and their HIV-related phenotypes were within the ranges of the above infected partners. All the EUI and HIV-1-infected individuals and 47 uninfected, age- and sex-matched healthy volunteers were enrolled from the Santa Maria Annunziata Hospital, Firenze, and the Luigi Sacco Hospital, Milano. All of the enrolees are Caucasians from the Toscana region. The ethics committees of the above hospitals have approved the research protocols. The genotyping analyses were approved by Kinki University School of Medicine. Written informed consent was obtained from all enrolees, and samples were anonymized and analyzed in a blinded fashion.

Phenotype definitions

Plasma HIV-1 load was quantified by using the AMPLICOR HIV Monitor test (Roche Diagnostic Systems, Nutley, New Jersey, USA) as described [4,6]. Possible presence of HIV-1 cDNA in PBMC and in cells

isolated by urethral swabbing or uterine cervical brushing was analyzed by a reverse transcription-PCR method [4,6]. For the detection of mucosal anti-HIV-1 IgA, 500 μl of mucus was collected from each enrolee by swabbing from the urethra or vagina [4,6]. Titers of serum anti-HIV antibodies were determined by an enzyme-linked immunosorbent assay (EIA) using Abbot HIV-1/2^+ test (Abbott Laboratories, Abbott Park, Illinois, USA). This assay detects HIV-specific IgG and IgM [7]. Titration of HIV-1-specific IgA in the mucosal secretions was performed by an isotype-specific EIA using the HIV EIA test (Calypte Biomedical Corp., Berkeley, California, USA) with modifications [4–9]. HIV-1-reactive memory T cells in the peripheral blood were enumerated by an enzyme-linked immunospot assay for interferon (IFN)-γ as described [6].

Analyses of human SSLP markers

Five-hundred nanograms of genomic DNA extracted from PBMC of each examined individual was used as the template for 40 cycles of PCR amplification using the flanking primer sets designed based on the sequence data compiled in the Ensembl Genome Browser (http://www.ensembl.org/) and ordered from QIAGEN GmbH. Each forward primer was labeled with a florescent dye, and 50–100 fmol of PCR amplified fragments were applied onto an ABI 3100 DNA sequencer (Applied Biosystems, Foster City, California, USA) with appropriate size markers. Peak identification and size measurements were done with the GeneScan software (Applied Biosystems). To determine absolute fragment sizes, PCR products obtained from two or more homozygotes for each locus were cloned into pCR2.1-TOPO vector (Invitorogen Life Technologies) and sequenced by using the M13 forward primer until six or more identical clones were observed for each allele.

Population genetic analyses and detection of linkage disequilibrium (LD)

Genotypic data were analyzed for possible population differentiation and LD between pairs of loci by using the Arlequin 2.001 (Genetics and Biometry Laboratory, University of Geneva, Switzerland). A population-pairwise genetic distance test using pairwise F_{ST} and extended exact test were performed to examine possible population differentiation. A likelihood ratio test was performed to examine the possible LD between pairs of loci. A total of 100,172 permutations on 10 initial conditions were performed by the expectation maximizing algorithm for each pair of loci.

Statistical analyses

Distributions of allele frequencies at each examined locus were compared between each pair of the three phenotypic groups by a Monte-Carlo approach using the CLUMP software [28]. T2 statistic was chosen because many cells in the contingency tables contained values ≤ 2.

To examine the possible presence of a dominant allele having different frequencies between the three phenotypic groups, mathematical analyses were performed based on the assumption that the number of individuals possessing each genotype had a multinominal distribution. Since the number of candidate dominant alleles was more than one, multiple comparisons were taken into consideration. The test statistics for alleles i and j, t_i and t_j, respectively, can be strongly correlated especially when most of the individuals having allele i or j are of the genotype i/j. Therefore, the typically used Bonferroni correction may be too conservative. A universally applicable method for overcoming this problem is a closed testing procedure [29], where t_i is based on a well-acquainted variance stabilizing transformation and the test statistic for a common hypothesis is based on the maximization of t_i's. To calculate the P-values, we applied a parametric bootstrap [30] based on the asymptotic null distribution of t_i's. Details of the mathematical methods are described in the Appendix section.

Results

Linkage mapping of a mouse locus controlling FV-neutralizing antibodies

When (B10.A × A/WySn)F_1 and A/WySn mice that share FV-susceptible *Fv-1*$^{b/b}$, *Fv-2*^{s}, and H2$^{a/a}$ genotypes were tested for their production of virus-neutralizing antibodies, none possessed a detectable level of neutralizing antibodies at post-infection day (PID) 10. Neutralizing antibodies remained undetectable at PID 15 and 20 in parental A/WySn mice. In contrast, all the infected (B10.A × A/WySn)F_1 mice possessed a significant neutralizing titer at PID 15, and the titers increased toward PID 20 (Fig. 1a). Therefore, possible segregation of neutralizing titers in (B10.A × A/WySn) × A/WySn backcross mice was examined by testing them at PID 15, 17, and 21. Virus-neutralizing antibodies were not detectable in 63 (44%) of the 143 backcross mice at PID 15 (Fig. 1b), suggesting that a single locus is involved in the production or lack of production of neutralizing antibodies. For linkage analyses, we concentrated genotyping on chromosome 15, because initial analyses performed by using 43 separate backcross individuals showed significant correlation between virus-neutralizing titers at PID 17 and genotypes at four loci in chromosome 15 (data not shown). The results of linkage analyses performed by using the 143 backcross mice indicated a strong correlation between genotypes at marker loci in chromosome 15 and titers of virus-neutralizing antibodies at PID 15, with the strongest correlation ($\chi^2 = 74.0$, $P = 1.17 \times 10^{-7}$) observed at the D15Mit71 locus (Fig. 2). Linkage mapping with MAPMAKER/EXP located a single locus determining the presence or absence of virus-neutralizing antibodies at PID 15

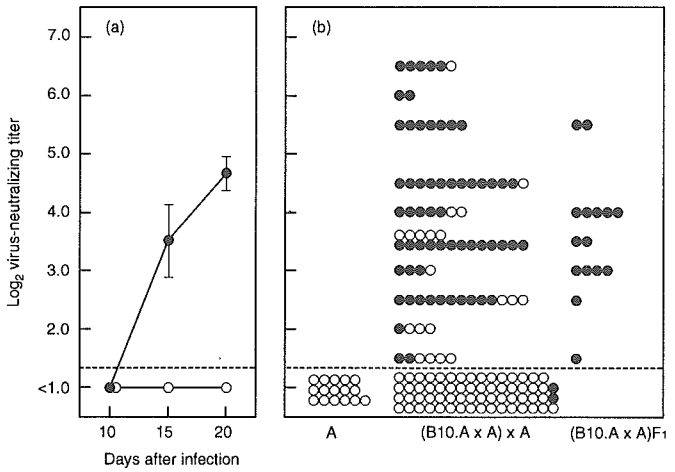

Fig. 1. Titers of virus-neutralizing antibodies in FV-infected mice. (a) Changes in the average titer ($n = 11–16$) of virus-neutralizing antibodies in (B10.A × A/WySn)F_1 (●) and A/WySn (○) mice at different time-points after infection with 150 spleen focus-forming units of FV. SEM. are shown with the bars. The dashed line indicates the limit of detection. (b) Titers of virus-neutralizing antibodies in each individual mouse tested at PID 15. Genotypes at the D15Mit71 locus are either homozygous for the A/WySn-derived allele (○) or heterozygous for the B10.A-derived and A/WySn-derived alleles (●).

between the D15Mit71 and D15Mit171 loci. Further mapping was performed by genotyping the backcross animals that possessed a critical recombination between the D15Mit28 and D15Mit171 loci. As a result, eight backcross mice that possessed reciprocal recombination within this region were identified (Fig. 2). Since a significant correlation ($P = 0.029$ by two-tailed Fisher's exact test) between genotypes at the D15Mit71, D15Mit2, D15Mit214, D15Mit69, and D15Mit70 loci and the production of virus-neutralizing antibodies at PID 15 was observed in these recombinant animals, it is conceivable that the locus controlling the production of FV-neutralizing antibodies is located within the region telomeric to the D15Mit1 and centromeric to D15Mit118 loci at the widest estimation.

Genetic analyses of HIV-1-exposed and uninfected Italians

The above region of mouse chromosome 15 harbors previously mapped genes that are known or likely to affect immune cell development and/or activation and retroviral replication. Therefore, we next explored the possibility that a putative ortholog of the above mouse locus might influence immune responsiveness in HIV-1 infection. Because of the route of transmission of HIV-1 and resultant rarity of multicase families, linkage analyses comparing affected and unaffected siblings are impossible. Thus, we performed a simple association study by comparing genotypes between the exposed but uninfected and HIV-1-infected individuals, hypothesizing that efficient anti-HIV-1 immune responses are associated with the presence of a dominant genetic factor which might be an ortholog of the above mouse locus conferring the ability to produce FV-neutralizing antibodies. Thus, the three phenotypically distinct groups of individuals (Table 1) were genotyped at the loci shown in Fig. 2. The examined groups were not different to each other when tested for population-pairwise genetic distance ($P > 0.17$), in accordance with their all being Caucasians enrolled from the Toscana region of Italy. When allele frequencies were compared among the three phenotypic groups, their distribution at the D22S277 locus differed between the EUI and healthy control groups at $P = 0.0396$. No significant difference was observed at the other loci. When likelihood ratio tests were performed for all possible pairs of the examined loci, a highly significant LD of an exact $P < 0.0004$ level was observed in all three groups between the D22S284, D22S423, and D22S299 loci, reflecting their close physical locations (Fig. 2 and Fig. 3). A similarly significant LD ($P < 0.00002$) was observed between the D22S418 and D22S1166 loci in all three groups, confirming their close genetic locations. Interestingly, a highly significant LD ($P < 0.00002$) was observed between the D22S276 and the above surrounding loci in both the HIV-1-infected and healthy control groups, but this was not observed in the EUI group (Fig. 3).

When frequencies of individuals possessing a particular allele at a given locus were compared among the three phenotypic groups by adopting a dominant model, objective mathematical analyses revealed multiple loci with significant differences (Table 2). These individual

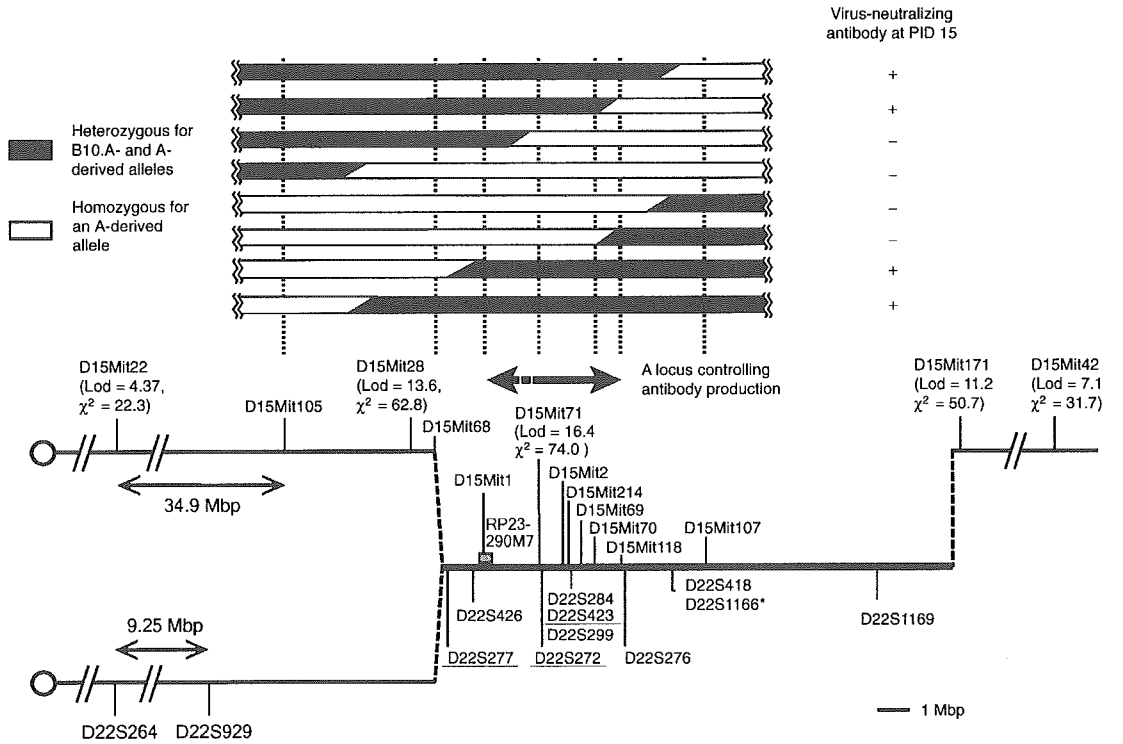

Fig. 2. The order of and distance between microsatellite markers located within the syntenic region of mouse chromosome 15 (the upper half of the diagram) and human chromosome 22 (the bottom half). Physical mapping and synteny data are based on those compiled in the Ensembl Genome Browser (http://www.ensembl.org/). Centromeres (○) are placed on the left. The mouse marker D15Mit28 has not been physically mapped, but genetic linkage data archived in the Mouse Genome Informatics site (http://www.informatics.jax.org) indicate that this locus, mapped at 43.7 cM, is closely linked to the D15Mit68 locus at 44.1 cM. Note that, although D15Mit1 is currently not included in the physical map of the mouse genome archived in the Ensembl Genome Browser, we identified the flanking primer and repeat sequences of this microsatellite marker (base numbers 47915-48097) within a clone of bacterial artificial chromosome, RP23-290M7, harbouring the segment of mouse chromosome 15 (shown with the hatched box). Lod scores and χ^2 values indicating degrees of genetic association between the identified genotypes and virus-neutralizing titers at PID 15 for each examined mouse locus are shown in parentheses. The estimated location of the putative mouse locus controlling the production of FV-neutralizing antibodies is shown with the bidirectional arrow. Human loci at which genotypes were compared between the EUI, HIV-infected, and healthy control groups are also shown, and the loci at which significant genetic differences were observed by the closed testing procedures are underlined. *The D22S1166 locus has not been physically mapped, but the genetic maps archived at the Center for Medical Genetics, Marshfield Clinic Research Foundation (http://research.marshfieldclinic.org/genetics/) indicate that this and the D22S418 loci are closely linked.

differences were further examined for possible false rejection of a single equal-frequency hypothesis due to multiple comparisons by using the closed testing procedure. As a result, frequencies of individuals possessing either the allele 156 or 158 at the D22S277 locus were significantly different between the EUI and two other groups, those of the individuals possessing the allele 134 at the D22S272 locus were significantly different between the EUI and healthy control groups, and those of individuals possessing the allele 229 at the D22S423 locus also differed significantly between the EUI and HIV-infected individuals.

Discussion

In the present study we have demonstrated that the presence or absence of virus-neutralizing antibodies in FV-infected (B10.A × A/WySn) × A/WySn backcross mice at PID 15 is closely associated with their genotypes at the chromosome 15 loci. The linkage mapping data indicated that a single gene controlling the production of virus-neutralizing antibodies was located near the D15Mit71 locus, colocalizing with the previously mapped *Rfv-3* locus [23,24]. Since the *Rfv-3*-associated phenotypes were defined by clearance of viremia by

Table 1. HIV-1-related phenotypes of the three groups genetically analyzed in the present study.

Group	Age	Plasma HIV load (copies/ml)	Urethral/ vaginal anti-HIV-1 IgA ($A_{405\ nm}$)	Serum anti-HIV-1 IgG ($A_{405\ nm}$)	HIV-1 envelope-reactive IFN-γ ELISPOT[a] (/10^6 cells)
HIV-1-exposed but uninfected ($n = 42$)	40.1 ± 1.4	Not detectable (all)[b]	0.556 ± 0.047[c] (0.12–1.14)[d]	0.004 ± 0.0006 (0.00–0.02)	131.2 ± 11.3[e] (5–280)
HIV-1-infected ($n = 49$)	40.8 ± 1.9	<40 – 750,000 (median: 400)[f]	0.360 ± 0.039 (0.11–0.87)	0.793 ± 0.069 (0.11–1.25)	63.4 ± 9.2 (<5–120)
Healthy control ($n = 47$)	37.8 ± 3.6	Not detectable (all)[b]	0.002 ± 0.0006 (0.00–0.03)	0.002 ± 0.0001 (0.00–0.01)	<5 (<5–15)

Numbers shown are mean ± SEM except for the Plasma HIV load.
[a]PBMC were stimulated with a mixture of five synthetic peptides representing the immunodominant and promiscuous epitopes identified in the HIV-1 gp160 [6], and spots of secreted interferon (IFN)-γ were visualized and counted by using a biotin-conjugated anti-IFN-γ antibody.
[b]All enrolees were tested for the presence of HIV genome by measuring plasma HIV-1 RNA and by detecting HIV-1 cDNA from total RNA of peripheral blood mononuclear cells. In the case of the exposed uninfected individuals (EUI), possible presence of HIV-1 cDNA was also tested in mucosal cells by reverse transcription–PCR. All the individuals in the EUI and healthy control groups were negative for all these tests.
[c]Significantly higher than the average for the HIV-1-infected individuals at $P = 0.0022$ by Welch's t test. A non-parametric analysis by Mann–Whitney's U-test also showed a significant difference, $P = 0.021$.
[d]Ranges of observed values are shown in parentheses for IgA and IgG titers and enzyme-linked immunospot (ELISPOT) foci.
[e]Significantly higher than the average for the HIV-1-infected individuals at $P = 0.015$ by Welch's t test, and $P = 0.0002$ by Mann–Whitney's U-test.
[f]All the HIV-1-infected individuals were enrolled during their chronic phase of infection before the initiation of antiretroviral drug treatment, but 32 of the 42 infected partners and the seven additional HIV-1-infected enrolees were receiving the highly active anti-retroviral therapy at the time of this study. The range of plasma viral load in the 13 currently untreated individuals in the infected group was 5900 to 750 000 (median, 65 000) copies/ml.

35–40 days after FV infection [22–25], and neutralizing antibodies were detectable at as early as PID 15 in mice possessing the B10.A-derived dominant allele (Fig. 1), it is conceivable that early production of virus-neutralizing antibodies is associated with early clearance of viremia.

It is intriguing that genotypes at microsatellite loci located within the segment of human chromosome 22 syntenic to mouse chromosome 15 differed between the HIV-1-exposed but uninfected and HIV-1-infected groups of individuals. The strongest association was observed at the D22S423 locus where the frequency of individuals possessing the allele 229 was significantly higher in the EUI group than in the HIV-1-infected one even after corrections for multiple comparisons were made. This marker locus is located in the middle of the chromosomal segment corresponding to the region of mouse chromosome 15 that harbors the gene locus controlling the production of virus-neutralizing antibodies (Fig. 2). It may also be worth noting that the alleles 156 and 158 at the D22S277 locus that are rare (5.6 and 9.3% per haploid chromosome, respectively) among the Caucasian CEPH

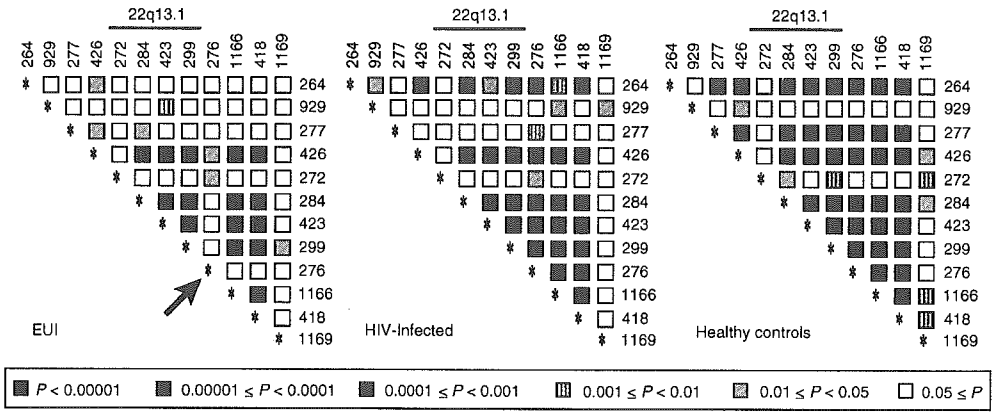

Fig. 3. Distributions of LD across chromosome 22. LD is plotted for the 12 microsatellite loci examined against each other, each represented by a small square. Locus names are abbreviated by omitting D22S. The pattern of distribution of LD is shown for each of the three phenotypic groups for comparison. Filling patterns reflect the significance level in exact P values as indicated at the bottom. The arrow indicates observed disruption within the segment of multilocus LD in the EUI group. The allele distributions in the three examined groups did not deviate from the Hardy-Weinberg equilibrium at any examined locus, except only at the D22S418 locus in the healthy control group, when exact tests using a Markov chain (100,172 chain length and 1,000 dememorization steps) were performed.

Table 2. Chromosome 22q association analyses.

Cytogenetic location	Locus	Allele size (bp)	Frequency in the EUI group[a]	Compared to[b]	Odds ratio	*P* value	
						Individual hypothesis	Common hypothesis
22q11.21	D22S264	188	0.405	HIV	3.276	0.0142	ns[c]
		198	0.238	HC	0.306	0.0128	ns
22q12.2	D22S277	158	0.310	HIV	3.766	0.0152	ns
		156 or 158	0.429	HIV	3.656	0.0066	0.0378[d]
				HC	3.875	0.0079	0.0448[d]
		162	0.262	HC	0.379	0.0371	ns
22q13.1	D22S272	134	0.667	HC	0.308	0.0243	0.0466[d]
22q13.1	D22S423	229	0.333	HIV	4.200	0.0087	0.0317[d]
22q13.2	D22S418	145	0.605	HC	2.520	0.0475	ns
	D22S1166	130	0.571	HC	2.816	0.0266	ns
22q13.32	D22S1169	126	0.643	HC	2.528	0.0313	ns

[a]Frequencies of individuals possessing the indicated allele either heterozygously or homozygously.
[b]HIV, HIV-1-infected individuals; HC, Healthy controls.
[c]Not significant (ns) at the $P < 0.05$ level.
[d]These differences are also significant ($P < 0.05$) after conventional Bonferroni correction.

population [31,32] were more frequently observed in the EUI group (9.5 and 17.9%, respectively). There were significant differences in the frequency of the allele 156 and that of the allele 158 ($P = 0.035$ and 0.0061, respectively, by two-tailed Fisher's exact test) when the HIV-1-infected and healthy control groups were combined and compared with the EUI group. The rates of microsatellite mutation are much higher than those of point mutation at coding genes [33], and the most common stepwise mutation is biased toward the reduction of repeat numbers for microsatellites of >20 repeats [34]. Thus, we can justifiably hypothesize that the alleles 156 and 158 at the D22S277 locus (25 and 26 dinucleotide repeats, respectively) are both linked to the same putative allele that is associated with the presence of immune responses to HIV-1 in the uninfected individuals. In this regard, the variance stabilizing analyses performed by assuming that the alleles 156 and 158 are both linked to a single dominant genetic factor resulted in the demonstration of significant differences between the EUI and HIV-1-infected, and the EUI and healthy control groups, and these individual null hypotheses were also rejected (significant difference validated) after the correction for multiple comparisons was made (Table 2). Further, when the same comparison was made between a combined group of the HIV-1-infected and healthy control individuals and the EUI group, the frequency of individuals possessing either the allele 156 or 158 was significantly higher among the EUI ($P = 0.0019$), and this was highly significant even after the correction for multiple comparisons was made ($P = 0.0121$). The combination of the HIV-1-infected and healthy control groups was justifiable because neither allele frequency distributions nor frequencies of individuals possessing the allele 156 or 158 were significantly different between the two groups. Thus, genotypes at multiple loci within the segment of human chromosome 22 that is syntenic to mouse chromosome 15 are significantly associated with the presence of strong mucosal and T-cell immune responses against HIV-1 (Table 1) in HIV-uninfected Italians. Furthermore, the multilocus LD spanning from D22S284 to D22S418 which is observed in both the HIV-infected and healthy control groups is disrupted at the D22S276 locus in the EUI group (Fig. 3). This observation is consistent with the hypothesis that in the ancestors of the EUI individuals a possible recombinational or mutational event might have happened in the chromosomal segment surrounding this locus.

Production and class-switching of virus-neutralizing antibodies in FV-infected mice are dependent on CD4 T-cell functions [26,27,35], and the priming of CD4 T-helper cells with a singe-epitope peptide resulted in the early production and class-switching of virus-neutralizing antibodies and strong protection against FV infection [20,27]. Likewise, EUI individuals enrolled into the present study possessed significantly higher amounts of mucosal anti-HIV-1 IgA and larger numbers of HIV-1 envelope-reactive T cells in the peripheral blood in comparison with the HIV-infected individuals (Table 1). IgA antibodies isolated from some EUI individuals have been shown to inhibit the replication of primary HIV-1 isolates [7] and HIV-1 transcytosis across the epithelial cells *in vitro* [8,36]. Thus, it is possible that efficient priming of T cells with HIV antigens might have resulted in rapid production of HIV-1-reactive IgA antibodies which, in turn, might have been involved in the possible immune protection in the EUI individuals. In this regard, it is noteworthy that IFN-γ production is required for the control of viremia and class-switching of virus-neutralizing antibodies in FV infected mice [37].

It has been shown that CD4 T cell-dependent early IgA responses against influenza virus infection can be generated in the absence of virus-specific IgM and IgG [38], and costimulatory signals required for mucosal IgA production are strikingly different from those needed for systemic antibody responses [39]. Similarly, mucosal IgA

responses to T-dependent HIV-1 antigens might be stimulated without inducing serum IgG production, and putative human homolog of the mouse gene influencing the T cell-dependent production of FV-neutralizing antibodies might be involved in the above activation of mucosal IgA-production in EUI individuals. In fact, the segment of mouse chromosome 15 between the D15Mit1 and D15Mit118 loci and the corresponding segment of human chromosome 22 harbor several genes that are known to be involved in T- and B-cell growth and activation. Expression analyses of these candidate genes both in the mouse model and in humans are currently underway.

None of the previously reported human genes that affect the risk of HIV acquisition are located in chromosome 22, *CCR5* and *CCR2* being located at 3p21, *SDF1* and *MBL2* at 10q11.1 and 10q11.2, respectively, *HLA* including the polymorphic *TNF* and *MIC* loci at 6p21.3, *KIR*s at 19q13.4, *IL10* at 1q31-32, and *SLC11A1 (NRAMP1)* at 2q35 [3,40–52]. In addition, the homozygous *CCR5-Δ32* mutation, which results in the lack of the HIV coreceptor [3,40–42], is known to be rare among the EUI individuals in Italy and Thailand [4,9,49], and was not found in the enrolees of the present study, although three of the 42 EUI individuals were heterozygous for this mutation (data not shown). In a very recent analysis of a separate cohort of repeatedly exposed but HIV-1-seronegative individuals in the USA, Liu *et al.* [53] demonstrated the lack of association between genotypes at the *CCR2*, *SDF1*, and *RANTES* loci and the uninfected status. The homozygous *CCR5-Δ32* mutation was also rare (3.2%) among the seronegative individuals. The same authors also noted a significant difference in the frequencies of heterozygosity at the polymorphic *DC-SIGN (CD209)* locus at 19p13.2 between the exposed but seronegative and HIV-1-infected groups: however, the observed frequency of heterozygotes was 3.2% (3/94), and thus, this genetic skewing could not explain the possible mechanisms that confer HIV resistance to the majority of the seronegative individuals. Altogether, our results have indicated the possible presence in human chromosome 22 of a novel genetic factor that is associated with strong T-cell and mucosal immune responses to HIV-1 antigens.

Acknowledgements

We thank M. P. Gorman and S. Tsuji-Kawahara for critically reading the manuscript.

Sponsorship: This work was supported in part by grants from the Ministry of Education, Culture, Sports, Science and Technology of Japan, including the High-Tech Research Center Project (2002), from the Ministry of Health, Labor and Welfare of Japan, from the Japan Health Science Foundation, from the Istituto Superiore di Sanita' "Programma Nazionale di Ricerca sull' AIDS", from Centro di Eccellenza CISI, from the EMPRO and AVIP EC WP6 Projects, and from the Tuscancy Region, General Drection, Right to Health and Solidarity Policy.

References

1. Rowland-Jones SL, McMichael A. **Immune responses in HIV-exposed seronegatives: Have they repelled the virus?** *Curr Opin Immunol* 1995; **7**:448–455.
2. Shearer GM, Clerici M. **Protective immunity against HIV infection: Has nature done the experiment for us?** *Immunol Today* 1996; **17**:21–24.
3. O'Brien SJ, Nelson GW, Winkler CA, Smith MW. **Polygenic and multifactorial disease gene association in man: Lessons from AIDS.** *Annu Rev Genet* 2000; **34**:563–591.
4. Mazzoli S, Trabattoni D, Lo Caputo S, Piconi S, Blé C, Meacci F, *et al.* **HIV-specific mucosal and cellular immunity in HIV-seronegative partners of HIV-seropositive individuals.** *Nature Med* 1997; **3**:1250–1257.
5. Kaul R, Trabattoni D, Bwayo JJ, Arienti D, Zagliani A, Mwangi F, *et al.* **HIV-1 specific mucosal IgA in a cohort of HIV-1-resistent Kenyan sex workers.** *AIDS* 1999; **13**:23–29.
6. Biasin M, Lo Caputo S, Speciale L, Colombo F, Racioppi L, Zagliani A, *et al.* **Mucosal and systemic immune activation is present in human immunodeficiency virus-exposed seronegative women.** *J Infect Dis* 2000; **182**:1365–1374.
7. Mazzoli S, Lopalco L, Salvi A, Trabattoni D, Lo Caputo S, Semplici F, *et al.* **Human immunodeficiency virus (HIV)-specific IgA and HIV neutralizing activity in the serum of exposed seronegative partners of HIV-seropositive persons.** *J Infect Dis* 1999; **180**:871–875.
8. Belec L, Ghys PD, Hocini H, Nkengasong JN, Tranchot-Diallo J, Diallo MO, *et al.* **Cervicovaginal secretory antibodies to HIV type 1 that block viral transcytosis through epithelial barriers in highly exposed HIV-1-seronegative African women.** *J Infect Dis* 2001; **184**:1412–1422.
9. Lo Caputo S, Trabattoni D, Vichi F, Piconi S, Lopalco L, Villa ML, *et al.* **Mucosal and systemic HIV-specific immunity in HIV-exposed but uninfected heterosexual males.** *AIDS* 2003; **17**:531–538.
10. Teich N, Wyke J, Mak T, Bernstein A, Hardy W. In: RNA Tumor Viruses, 2nd edn. Edited by Weiss R, Teich N, Varmus H, Coffin J. New York: Cold Spring Harbor Laboratory; 1982: 785–998.
11. Kabat D. **Molecular biology of Friend viral erythroleukemia.** *Curr Top Microbiol Immunol* 1989; **148**:1–42.
12. Chesebro B, Miyazawa M, Britt WJ. **Host genetic control of spontaneous and induced immunity to Friend murine retrovirus infection.** *Annu Rev Immunol* 1990; **8**:477–499.
13. Hoatlin ME, Kabat D. **Host-range control of a retroviral disease: Friend erythroleukemia.** *Trends Microbiol* 1995; **3**:51–57.
14. Best S, Le Tissier P, Towers G, Stoye JP. **Positional cloning of the mouse retrovirus restriction gene Fv1.** *Nature* 1996; **382**:826–829.
15. Persons DA, Paulson RF, Loyd MR, Herley MT, Bodner SM, Bernstein A, *et al.* **Fv2 encodes a truncated form of the Stk receptor tyrosine kinase.** *Nat Genet* 1999; **23**:159–165.
16. Ikeda H, Laigret F, Martin MA, Repaske R. **Characterization of a molecularly cloned retroviral sequence associated with Fv-4 resistance.** *J Virol* 1985; **55**:768–777.
17. Ikeda H, Sugimura H. **Fv-4 resistance gene: a truncated endogenous murine leukemia virus with ecotropic interference properties.** *J Virol* 1989; **63**:5405–5412.
18. Miyazawa M, Nishio J, Chesebro B. **Genetic control of T cell responsiveness to the Friend murine leukemia virus envelope antigen. Identification of the class II loci of H-2 as immune response genes.** *J Exp Med* 1988; **168**:1587–1605.
19. Iwashiro M, Kondo T, Shimizu T, Yamagishi H, Takahashi K, Matsubayashi Y, *et al.* **Multiplicity of virus-encoded helper T-cell epitopes expressed on FBL-3 tumor cells.** *J Virol* 1993; **67**:4533–4542.

20. Sugahara D, Tsuji-Kawahara S, Miyazawa M. **Identification of a protective CD4+ T-cell epitope in p15gag of Friend murine leukemia virus and role of the MA protein targeting the plasma membrane in immunogenicity.** *J Virol* 2004; **78**:6322–6334.
21. Peterson KE, Iwashiro M, Hasenkrug KJ, Chesebro B. **Major histocompatibility complex class I gene controls the generation of gamma interferon-producing CD4+ and CD8+ T cells important for recovery from Friend retrovirus-induced leukemia.** *J Virol* 2000; **74**:5363–5367.
22. Chesebro B, Wehrly K. **Studies on the role of the host immune response in recovery from Friend virus leukemia. I. Antiviral and antileukemia cell antibodies.** *J Exp Med* 1976; **143**:73–84.
23. Hasenkrug KJ, Valenzuela A, Letts V, Nishio J, Chesebro B, Frankel WN. **Chromosome mapping of Rfv3, a host resistance gene to Friend murine retrovirus.** *J Virol* 1995; **69**:2617–2620.
24. Super HJ, Hasenkrug KJ, Simmons S, Brooks DM, Konzek R, Sarge KD, *et al.* **Fine mapping of the Friend retrovirus resistance gene, Rfv3, on mouse chromosome 15.** *J Virol* 1999; **73**:7848–7852.
25. Doig D, Chesebro B. **Anti-Friend virus antibody is associated with recovery from viremia and loss of viral leukemia cell-surface antigens in leukemic mice. Identification of Rfv-3 as a gene locus influencing antibody production.** *J Exp Med* 1979; **150**:10–19.
26. Miyazawa M, Nishio J, Wehrly K, Chesebro B. **Influence of MHC genes on spontaneous recovery from Friend retrovirus-induced leukemia.** *J Immunol* 1992; **148**:644–646.
27. Miyazawa M, Fujisawa R, Ishihara C, Takei YA, Shimizu T, Uenishi H, *et al.* **Immunization with a single T helper cell epitope abrogates Friend virus-induced early erythroid proliferation and prevents late leukemia development.** *J Immunol* 1995; **155**:748–758.
28. Sham PC, Curtis D. **Monte Carlo tests for association between disease and alleles at highly polymorphic loci.** *Ann Hum Genet* 1995; **59**:97–105.
29. Hsu JC. *Multiple comparisons: theory and methods.* New York: Chapman & Hall/CRC; 1996.
30. Hall P. *The bootstrap and edgeworth expansion.* New York: Springer; 1992.
31. Weissenbach J, Gyapay G, Dib C, Vignal A, Morissette J, Millasseau P, *et al.* **A second-generation linkage map of the human genome.** *Nature* 1992; **359**:794–801.
32. Gyapay G, Morissette J, Vignal A, Dib C, Fizames C, Millasseau P, *et al.* **The 1993–94 Genethon human genetic linkage map.** *Nat Genet* 1994; **7**:246–339.
33. Li Y-C, Korol AB, Fahima T, Beiles A, Nevo E. **Microsatellites: genetic distribution, putative functions and mutational mechanisms: a review.** *Mol Ecol* 2002; **11**:2453–2465.
34. Whittaker JC, Harbord RM, Boxall N, Mackay I, Dawson G, Sibly RM. **Likelihood-based estimation of microsatelliote mutation rates.** *Genetics* 2003; **164**:781–787.
35. Super HJ, Brooks D, Hasenkrug K, Chesebro B. **Requirement for CD4+ T cells in the Friend murine retrovirus neutralizing antibody response: evidence for functional T cells in genetic low-recovery mice.** *J Virol* 1998; **72**:9400–9403.
36. Devito C, Broliden K, Kaul R, Svensson L, Johansen K, Kiama P, *et al.* **Mucosal and plasma IgA from HIV-1-exposed uninfected individuals inhibit HIV-1 transcytosis across human epithelial cells.** *J Immunol* 2000; **165**:5170–5176.
37. Dittmer Y, Peterson KE, Messer R, Stromnes IM, Race B, Hasenkrug KJ. **Role of interleukin-4 (IL-4), IL-12, and gamma interferon in primary and vaccine-induced immune responses to Friend retrovirus infection.** *J Virol* 2001; **75**:654–660.
38. Sangster MY, Riberdy JM, Gonzalez M, Topham DJ, Baumgarth N, Doherty PC. **An early CD4+ T cell-dependent immunoglobulin A responses to influenza infection in the absence of key cognate T-B interactions.** *J Exp Med* 2003; **198**:1011–1021.
39. Gärdby E, Wrammert J, Schön K, Ekman L, Leandersen T, Lycke N. **Strong differential regulation of serum and mucosal IgA responses as revealed in CD28-deficient mice using cholera toxin adjuvant.** *J Immunol* 2003; **170**:55–63.
40. Dean M, Carrington M, Winkler C, Huttley GA, Smith MW, Allikmets R, *et al.* **Genetic restriction of HIV-1 infection and progression to AIDS by a deletion allele of the CCR5 structural gene.** *Science* 1996; **273**:1856–1862.
41. Liu R, Paxton WA, Choe S, Ceredini D, Martin SR, Horuk R, *et al.* **Homozygous defect in HIV-1 coreceptor accounts for resistance of some multiply-exposed individuals to HIV-1 infection.** *Cell* 1996; **86**:367–377.
42. Samson M, Libert F, Doranz BJ, Rucker J, Liesnard C, Farber CM, *et al.* **Resistance to HIV-1 infection in Caucasian individuals bearing mutant alleles of the CCR-5 chemokine receptor gene.** *Nature* 1996; **382**:722–725.
43. Martin MP, Dean M, Smith MW, Winkler C, Gerrard B, Michael NL, *et al.* **Genetic acceleration of AIDS progression by a promoter variant of CCR5.** *Science* 1998; **282**:1907–1911.
44. Smith MW, Dean M, Carrington M, Winkler C, Huttley GA, Lomb DA, *et al.* **Contrasting genetic influence of CCR2 and CCR5 receptor gene variants on HIV-1 infection and disease progression.** *Science* 1997; **277**:959–965.
45. Winkler C, Modi W, Smith MW, Nelson GW, Wu X, Carrington M, *et al.* **Genetic restriction of AIDS pathogenesis by an SDF-1 chemokine gene variant.** *Science* 1998; **279**:389–393.
46. Carrington M, Nelson G, Martin MP, Kissner T, Vlahov D, Goedert JJ, *et al.* **HLA and HIV: Heterozygote advantage and B*35-Cw*04 disadvantage.** *Science* 1999; **3**:1748–1752.
47. Shin HD, Winkler C, Stephens JC, Bream J, Young H, Goedert JJ, *et al.* **Genetic restriction of HIV-1 infection and AIDS progression by promoter alleles of interleukin 10.** *Proc Natl Acad Sci U S A* 2000; **97**:14467–14472.
48. Martin MP, Gao X, Lee J-H, Nelson GW, Detels R, Goedert JJ, *et al.* **Epistatic interaction between KIR3DS1 and HLA-B delays the progression to AIDS.** *Nat Genet* 2002; **31**:429–434.
49. Beyrer C, Artenstein AW, Rugpao S, Stephens H, Van Cott TC, Robb ML, *et al.* **Epidemiologic and biologic characterization of a cohort of human immunodeficiency virus type 1 highly exposed, persistently seronegative female sex workers in northern Thailand.** *J Infect Dis* 1999; **79**:59–68.
50. Delgado JC, Leung JY, Baena A, Clavijo OP, Vittinghoff E, Buchbinder S, *et al.* **The −1030/−862-linked TNF promoter single-nucleotide polymorphisms are associated with the inability to control HIV-1 viremia.** *Immunogenetics* 2003; **55**: 497–501.
51. Garred P, Madsen HO, Balslev U, Hofmann B, Pedersen C, Gerstoft J, *et al.* **Susceptibility to HIV infection and progression of AIDS in relation to variant alleles of mannose-biding lectin.** *Lancet* 1997; **349**:236–240.
52. Marquet S, Sánchez F, Arias M, Rodríguez J, París SC, Skamene E, *et al.* **Variations of the human NRAMP1 gene and altered human immunodeficiency virus infection susceptibility.** *J Infect Dis* 1999; **180**:1521–1525.
53. Liu H, Hwangbo Y, Holte S, Lee J, Wang C, Kaupp N, *et al.* **Analysis of genetic polymorphisms in CCR5, CCR2, stromal cell-derived factor-1, RANTES, and dendritic cell-specific intercellular adhesion molecule-3-grabbing nonintegrin in seronegative individuals repeatedly exposed to HIV-1.** *J Infect Dis* 2004; **190**:1055–1058.

Appendix

The possible presence of a dominant allele having different frequencies between the phenotypic groups was examined as follows: Define x_{ij} as the number of individuals having the genotype i/j $(i \leq j)$ for the EUI group, where $n = \sum_{i \leq j} x_{ij}$ is the total number of individuals belonging to this group. Assume that $x = (x_{ij})_{i \leq j}$ has a multinomial distribution with the parameter $a = (a_{ij})_{i \leq j}$, where $\sum_{i \leq j} a_{ij} = 1$. For convenience, let $a_{ji} = a_{ij}$. Similarly, define the notations y, b and z, c for the HIV-1-infected and healthy control groups, respectively. The frequency of the individuals having the allele i for the EUI group is expressed as $a_i = \sum_k a_{ik}$. Similarly, define b_i and c_i. The hypothesis where the frequencies of the individuals having the allele i for the EUI and HIV-infected groups is the same is expressed

as H_i: $a_i = b_i$. Similarly, consider the hypothesis $a_i = c_i$ to compare the EUI with healthy control groups.

We tested whether or not the frequency of individuals possessing a certain dominant allele in the EUI group was different from those in other groups. Since there are multiple candidate alleles at each locus, we must take multiple comparisons into consideration. Let t_i be the test statistic for allele i. t_i and t_j can be strongly correlated, especially when most of the individuals having allele i or j are of the genotype i/j. Therefore, the typically used Bonferroni correction can be too conservative. A universally applicable method for overcoming this problem is a closed testing procedure [29], where t_i is based on a well-acquainted variance stabilizing transformation and the test statistic for a common hypothesis is based on the maximization of t_i values.

Let $\overline{H}$ be the closed set consisting of all the intersections of the hypotheses' H_i values. Assume that we can make the reject region with common significance level α for any hypothesis $H \in \overline{H}$. The closed testing procedure says that we can reject $H \in \overline{H}$ only after we reject all the hypotheses including H, using the corresponding reject region. Let t_i be the standardized test statistic for the hypothesis H_i. The corresponding reject region becomes $W_i = \{|t_i| > e_i\}$. Consider a common hypothesis H. For example, let H be the intersection of $H_1, \ldots, H_I$. The corresponding reject region can be defined by $W = \{\max_{i=1,\ldots,I}|t_i| > e\}$. We used the following variance stabilizing type as the standardized test statistic:

$$t_i = \frac{\left(\sin^{-1}\sqrt{x_i/n_x} - \sin^{-1}\sqrt{y_i/n_y}\right)}{\sqrt{1/4n_x + 1/4n_y}}$$

where $n_x = \sum_{i \le j} x_{ij}$ and $n_y = \sum_{i \le j} y_{ij}$. As an advantage over the commonly used likelihood ratio and Pearson's χ^2 tests, the above type enables us to infer that the smaller a P value is the stronger the rejection of the corresponding null hypothesis, because the variances of the arcsine are constant independent of the samples. In view of the closed testing procedure, if the maximal intersection hypothesis $H \in \overline{H}$ is rejected, the individual hypothesis corresponding to the minimum P value can automatically be rejected. In addition, if the hypothesis corresponding to the minimum P value alone is rejected among the individual hypotheses, it is the only rejected hypothesis.

The joint distribution of t_i values can be approximated by the multivariate normal distribution under the null hypothesis, and the corresponding approximated P values can easily be calculated for the individual hypotheses. The approximated P values for a common hypothesis can be calculated by using the central limit theorem and the parametric bootstrap [30] based on the asymptotic null distribution of t_i values. To avoid unnecessary disturbances, we tested only the hypotheses having the estimated frequency ≥ 0.1 when considering the common hypotheses, because alleles with a frequency < 0.1 cannot explain the phenotype of the whole group. Calculations were performed by drawing 100 000 random samples from the approximated multivariate normal distribution for each hypothesis.

International Immunology, Vol. 18, No. 1, pp. 183–198
doi:10.1093/intimm/dxh361

Peptide-induced immune protection of CD8$^+$ T cell-deficient mice against Friend retrovirus-induced disease

Hiroyuki Kawabata[1], Atsuko Niwa[1,3], Sachiyo Tsuji-Kawahara[1], Hirohide Uenishi[2], Norimasa Iwanami[1,4], Hideaki Matsukuma[1], Hiroyuki Abe[1], Nobutada Tabata[1,5], Haruo Matsumura[1] and **Masaaki Miyazawa[1]**

[1]Department of Immunology, Kinki University School of Medicine, 377-2 Ohno-Higashi, Osaka-Sayama, Osaka 589-8511, Japan
[2]Genome Research Department, National Institute of Agrobiological Science, Tsukuba, Ibaraki 305-8602, Japan

[3]Present address: Department of Pharmacology, Kinki University School of Medicine, Osaka-Sayama, Osaka 589-8511, Japan
[4]Present address: Division of Experimental Immunology, Institute for Genome Research, University of Tokushima, Tokushima 770-8503, Japan
[5]Present address: Department of Pediatrics, Kinki University School of Medicine, Osaka-Sayama, Osaka 589-8511, Japan

Keywords: B cell-deficient, β_2-microglobulin-deficient, CD4$^+$ T, epitope, vaccine

Abstract

CD8$^+$ CTLs and virus-neutralizing antibodies have been associated with spontaneous and vaccine-induced immune control of retroviral infections. We previously showed that a single immunization with an *env* gene-encoded CD4$^+$ T cell epitope protected mice against fatal Friend retrovirus infection. Here, we analyzed immune cell components required for the peptide-induced anti-retroviral protection. Mice lacking CD8$^+$ T cells were nevertheless protected against Friend virus infection, while mice lacking B cells were not. Virus-producing cells both in the spleen and bone marrow decreased rapidly in their number and became undetectable by 4 weeks after infection in the majority of the peptide-immunized animals even in the absence of CD8$^+$ T cells. In the vaccinated animals the production and class switching of virus-neutralizing and anti-leukemia cell antibodies were facilitated; however, virus-induced erythroid cell expansion was suppressed before neutralizing antibodies became detectable in the serum. Further, the numbers of virus-producing cells in the spleen and bone marrow in the early stage of the infection were smaller in the peptide-immunized than in unimmunized control mice in the absence of B cells. Thus, peptide immunization facilitates both early cellular and late humoral immune responses that lead to the effective control of the retrovirus-induced disease, but CD8$^+$ T cells are not crucial for the elimination of virus-infected cells in the peptide-primed animals.

Introduction

Understanding the types of immune responses associated with and responsible for effective control of viral infection is pivotal for the development of antiviral vaccines. We, along with other researchers, have been studying the requirements of different immune cell components and their regulation by host genetic factors utilizing the mouse model of Friend retrovirus infection. Friend retrovirus complex (FV) is composed of replication-competent Friend murine leukemia virus (F-MuLV) and defective spleen focus-forming virus (SFFV), the latter of which induces rapid growth and terminal differentiation of infected erythroid progenitor cells (1, 2). FV is known to induce fatal erythroleukemia associated with severe immunosuppression when inoculated into immunocompetent adult mice of susceptible strains (1, 3). Genotypes at both MHC class I and class II loci, along with those at a non-MHC locus located on chromosome 15, affect spontaneous immune resistance against FV-induced disease development which is phenotypically manifested by the regression of early splenomegaly and clearance of viremia (1, 4–8). As predicted, requirements of both CD4$^+$ and CD8$^+$ T cells for the above

Correspondence to: M. Miyazawa; E-mail: masaaki@med.kindai.ac.jp

Transmitting editor: K. Sugamura

Received 4 June 2005, *accepted* 28 October 2005

Advance Access publication 13 December 2005

spontaneous resistance have been demonstrated through antibody-mediated depletion of T cell subsets and through the blocking of T cell responses by administration of anti-MHC class II antibodies (9, 10). Further, different roles of $CD4^+$ and $CD8^+$ T cells and of virus-neutralizing antibodies have been demonstrated for immune protection against FV infection induced with a live attenuated vaccine (11, 12).

We previously showed that a single immunization with an 18-mer peptide that contains a single $CD4^+$ T cell epitope identified within the *env* gene product SU of F-MuLV induces strong protective immunity against fatal FV infection in susceptible strains of mice (13, 14). In peptide-immunized (B10.A × A.BY)F_1 mice, the vast majority of virus-producing cells were eliminated from the spleen between 8 and 12 days after FV challenge, and the SFFV-induced early splenomegaly regressed rapidly. Production and class switching of virus-neutralizing antibodies roughly coincided with the above reduction in the number of virus-producing cells in the spleen (13), suggesting the possible importance of virus-neutralizing antibodies in the vaccine-induced confinement of FV infection. However, since the activation of both $CD4^+$ and $CD8^+$ cytotoxic effector cells and of NK cells was detectable prior to the decrease of virus-producing cells in peptide-immunized (BALB/c × C57BL/6)F_1 ($CB6F_1$) mice (14), it was also possible that the cellular responses, rather than the antibodies, were mainly responsible for the control of FV-induced disease development conceivably through the destruction of virus-producing cells. Moreover, since $CD8^+$ CTLs and NK cells were activated in comparable degrees both in peptide-immunized and unimmunized animals after FV infection (14), their actual extents of contribution to the peptide-induced immune protection remained unclear.

To directly evaluate the role of each separate immune cell component in peptide-induced protection against FV infection and to compare the effector mechanisms induced by the peptide immunization with those induced by previously described live attenuated vaccines (11, 15), we performed the protection experiments on the highly susceptible strain of mice that lacked either $CD8^+$ T or B lymphocytes.

Methods

Mice

BALB/c-AJcl and $CB6F_1$ mice were purchased from Japan SLC, Inc., Hamamatsu, Japan. (B10.A × A.BY)F_1 mice were those described previously (13). Breeding pairs of BALB/c-J-*B2m*^{tm1Unc} and C57BL/6J (B6)-*B2m*^{tm1Unc} mice carrying homozygous disruption of the β_2-microglobulin gene ($\beta_2 m^{-/-}$) were purchased from the Jackson Laboratory, Bar Harbor, ME, USA, and F_1 crosses were produced at the Animal Facilities, Kinki University School of Medicine. Phenotypic lack of $CD8^+$ T cells in the produced F_1 crosses was confirmed by bleeding each mouse from the tail vein and staining peripheral blood with a mixture of fluorescence-labeled anti-CD4 and anti-CD8 mAbs as described in the following section.

B6-*Igh-6*^{tm1Cgm} mice carrying homozygous disruption of the membrane exon of the Ig μ-chain gene (μ-chain membrane exon-targeted: *μMT/μMT*) and thus lacking B cells (16) were also purchased from the Jackson Laboratory. To introduce the μ-chain disruption into BALB/c background, a cross-intercross production of a congenic strain was performed as follows: the B cell-deficient B6 male mice were mated with BALB/c female mice and F_1 crosses carrying heterozygous disruption of the μ-chain membrane exon were obtained. These heterozygous F_1 crosses were cross-mated, and F_2 mice carrying the homozygous μ gene disruption were selected by performing both genetic and phenotypic analyses as described below. The homozygous disruption of the μ-chain membrane exon in the resulting F_2 crosses was confirmed by PCR analyses as follows: genomic DNA was prepared from the tail tip of each mouse using DNeasy Tissue Kit (Qiagen GmbH, Hilden, Germany) according to the manufacturer's instructions. Oligo-DNA primers (5′ primer: 5′-TCTATCGCCTTCTTGACGAG-3′, 3′ primer: 5′-TACAGCTCAGCTGTCTGTGG-3′) were prepared based on the sequence information on the knockout cassette (16) and were used for PCR amplification of genomic DNA fragments. PCR products were separated by electrophoresis in a 4% agarose gel and were visualized under a UV light after ethidium bromide staining. In addition to the above genetic analyses, peripheral blood was stained with a mixture of fluorescence-labeled anti-CD3 and anti-CD19 mAb, and multicolor flow cytometric analyses were performed as described in the following section. Male F_2 mice carrying homozygous disruption of the μ-chain membrane exon and thus lacking B cells were mated with BALB/c female mice again, and this cross-intercross mating procedure was repeated seven times. After the seventh cycle of crossing and intercrossing, the resultant BALB/c-background mice possessing homozygous disruption of the μ-chain gene were maintained by sister–bother mating, and $CB6F_1$ mice lacking B cells were produced by crossing the B6-*Igh-6*^{tm1Cgm} and the above-established BALB/c-*μMT/μMT* mice.

For immune protection experiments, both male and female mice aged 8–11 weeks at the time of immunization were used throughout the present study. All the animal experiments were approved by the Animal Experiment Committee and performed under the guidelines of Kinki University.

Viruses and their inoculation

A stock of B-tropic FV complex was originally given by Bruce Chesebro, Laboratory of Persistent Viral Diseases, National Institute of Allergy and Infectious Diseases, Hamilton, MT, USA. The stock used in the present study has been described (14, 17). SFFV and F-MuLV titers of the FV stock were determined as described previously (13, 18). For inoculation into $CB6F_1$ mice, a dilution of the virus stock prepared with phosphate-buffered balanced salt solution (PBBS) containing 2% fetal bovine serum (FBS) was injected intravenously into the tail vein. Infected mice were observed at least twice a day and the number of surviving mice was determined. The development of splenomegaly was monitored by palpation as described (5, 17, 19). In some experiments, moribund mice were killed by cervical dislocation and spleen weights were measured to compare the results of palpation with actual spleen weights. Spleens weighing >0.5 g were consistently marked as palpable splenomegaly. Mice found dead were

dissected, and their spleen weight was measured to confirm leukemic death.

Peptide synthesis and immunization

The peptides used for detailed mapping of the $CD4^+$ T cell epitope were synthesized by Fmoc chemistry and purified, and their molecular weight confirmed by quad-polar mass spectrometry as described previously (20–22). Peptides used for immune protection experiments were ordered from Qiagen K. K. (Tokyo, Japan). For immunization each peptide was dissolved in PBBS and emulsified with an equal volume of CFA (Difco Laboratories, Detroit, MI, USA). Mice were injected intradermally with 100 μl of the emulsion given as multiple split doses into the abdominal wall. Control mice were given an emulsion of PBBS and CFA that did not contain any peptide.

T cell proliferation assays

Two T cell clones, F5-5 and FP7-11 (20, 23), specific for the $E^{b/d}$-restricted C-terminal epitope of F-MuLV *env* gene product were maintained as described previously (20). For examination of proliferative responses, 2×10^5 spleen cells irradiated with 40 Gy γ-ray were mixed with 2×10^5 T cells and various concentrations of a peptide in a well of 96-well microculture plates. After 48 h of incubation at 37°C, each culture was pulsed with 18.5 kBq [^{3}H]thymidine (Du Pont NEN, Boston, MA, USA) for the final 18 h. Cells were harvested onto a glass fiber filter, and incorporated radioactivity was measured with a microplate scintillation counter (TopCount, Packard Instrument Co., Meriden, CT, USA). For the calculation of relative stimulatory effect of each peptide, the concentration of peptide i (μM) required to induce 50% of the maximum proliferative response (ED_{50}) was divided with ED_{50} (μM) of the peptide in question (22, 23). In the present study proliferative responses were measured for a range of peptide concentrations between 0.01 and 20 μM in 2-fold dilutions, and peak responses (>30 000 counts per minute) were observed by stimulation with 1 μM of peptide i. ED_{50} of peptide i was 0.2 μM.

Assays for virus-neutralizing antibodies

The *in vitro* assays for quantitative measurement of F-MuLV-neutralizing antibodies have been described elsewhere in detail (5, 13, 17, 19). Mice were bled from the tail vein under ether anesthesia and sera separated were stored at −30°C until use. Stock of an infectious molecular clone of F-MuLV, FB29 (24), was prepared from a high-producer clone of chronically infected *Mus dunni* cells. Serial 2-fold dilutions of sera were made with PBBS containing 1% FBS and mixed with an appropriate dilution of the F-MuLV stock and inoculated to *Mus dunni* cells in 24-well plates. Control wells were inoculated with the virus dilution admixed with the diluent alone. Two days later, foci of F-MuLV-infected cells were visualized with mAb 720 (18) and counted under a dissecting microscope. Neutralizing titers were determined by the reciprocals of maximum dilutions that gave a reduction in the number of F-MuLV-infected cell foci to <25% of those in the control wells. IgG titers were determined by treating each serum sample with 0.05 M 2-mercaptoethanol whereas IgM titers were calculated by dividing the neutralizing titers of the untreated sera by the corresponding IgG titers (6).

Infectious center assays

These assays were performed as described previously (13, 17). Briefly, spleen and bone marrow cell suspensions prepared from mice challenged with FV were serially diluted with PBBS containing 2% FBS, plated in triplicate at concentrations between 30 and 3×10^6 cells per well onto monolayers of *Mus dunni* cells that had been seeded at 1.0×10^4 cells ml^{-1} per well on the previous day and then co-cultured for 2 days. After washing with PBBS and fixation with methanol, F-MuLV-infected cell foci were stained with mAb 720 (18), visualized by using the avidin-biotinylated peroxidase complex (Vector Laboratories, Burlingame, CA, USA) and counted under a magnifier. The numbers of detected foci are in linear correlation with the numbers of spleen cells inoculated in the range between 30 and 3×10^6 cells per well. For the plating of the whole spleen cells from each mouse, 5×10^6 spleen cells per well were added similarly to the previously started culture of *Mus dunni* cells in 20 wells of a 24-well plate, and the remaining spleen cells were diluted and plated at 5×10^5 and 5×10^4 cells per well into separate wells.

Flow cytometry

Flow cytometric analyses of cell-surface markers were performed as described elsewhere (14, 17, 25). Spleen and bone marrow tissues were dissociated in PBBS containing 2% FBS, and a single-cell suspension was prepared by passing each dissociated tissue through a nylon mesh. Cells were stained with a combination of the following mAbs, washed three times with PBBS containing 2% FBS and 0.05% NaN_3 and stained with 20 μg ml^{-1} 7-aminoactinomycin D (7-AAD). 7-AAD was used to exclude dead cells (26). The mAbs and their final concentrations used in the present study were: cychrome-conjugated anti-mouse CD3 (hamster IgG, PharMingen, San Diego, CA, USA) at 0.5 μg per 10^6 cells, FITC-conjugated anti-mouse CD4 (rat IgG2b, Seikagaku Corporation, Tokyo, Japan) at 0.5 μg per 10^6 cells, R-PE-conjugated anti-mouse CD8 (rat IgG2a, Caltag Laboratories, Burlingame, CA, USA) at 1 μg per 10^6 cells, PE-conjugated anti-mouse CD19 (rat IgG2a, PharMingen) at 1 μg per 10^6 cells, FITC-conjugated anti-mouse CD69 (hamster IgG, PharMingen) at 1 μg per 10^6 cells and allophycocyanin-conjugated anti-mouse TER-119 (PharMingen) at 0.2 μg per 10^6 cells. TER-119 reacts with a molecule associated with glycophorin A, and marks the late erythroblasts and mature erythrocytes, but not burst-forming and colony-forming units of erythroid cells (27). Biotinylated mAb 720 (IgG1) and 514 (IgM) used for the detection of F-MuLV gp70 and SFFV gp55, respectively, on infected cell surfaces has been described (13, 17). mAb 34 (IgG2b) reactive with the p15 (MA) protein (28) was similarly purified and biotinylated to detect cell-surface expression of the *gag* gene products (19). All staining reactions were performed in the presence of 0.25 μg per 10^6 cells anti-mouse CD16/CD32 (PharMingen) as described previously (25) to prevent the binding of mAb to FcR-expressing cells. Isotype-matched control antibodies were either purchased from the same suppliers or prepared as purified and biotinylated Ig of an irrelevant specificity as described (25), and staining patterns obtained with the negative-control antibodies were used to draw demarcation lines between cells positively stained and

those not stained. Multicolor flow cytometric analyses were performed with a Becton Dickinson FACSCalibur and CellQuest software (Becton Dickinson Immunocytometry Systems, San Jose, CA, USA). Mature erythrocytes and dead cells were excluded from the analyses by setting a polygonal gate in the dot plots showing intensities of forward scatter and fluorescence for 7-AAD.

Titration of serum antibody reactive to the surface of FV-induced leukemia cells

Sera were serially diluted between 1/4 and 1/256 with PBBS and 100 μl of each dilution was incubated with 10^6 FV-induced leukemia cells Y57-2C ($H2^{b/b}$). Characteristics of the leukemia cell line used in the present study have been described (14). After washing twice with PBBS containing 2% FBS, bound IgM and IgG were differentially detected by incubating the cells either with FITC-conjugated anti-mouse IgM (μ-chain specific, Southern Biotechnology Associates, Inc., Birmingham, AL, USA) at 5 μg per 10^6 cells or with FITC-conjugated anti-mouse IgG (γ-chain specific, Zymed Laboratories, Inc., South San Francisco, CA, USA) at 1.5 μg per 10^6 cells, respectively, for 20 min. Stained cells were washed three times before being examined by flow cytometry as described above.

Purification of T cells and their transfer

Purification of T cell subsets from the spleen of naive, immunized and/or FV-infected mice was performed by using mAb-conjugated magnetic microbeads and a magnetic cell sorter I (Miltenyi Biotec GmbH, Bergisch Gladbach, Germany) according to the manufacturer's instructions. Spleen cells were first treated with Tris-buffered ammonium chloride solution to lyse erythrocytes, and incubated with anti-B220 mAb-conjugated magnetic beads to remove B cells by passing through a negatively selecting CS column. To purify $CD4^+$ T cells, $B220^-$ cells were then incubated with anti-CD8 mAb-conjugated magnetic beads, passed through a CS column to remove $CD8^+$ cells and then incubated with anti-CD4 mAb-conjugated microbeads to positively select $CD4^+$ cells by passing through a VS column. Multicolor flow cytometric analyses revealed that the resultant cell preparation was >99% $CD4^+$. $CD8^+$ cells were similarly purified from $B200^-$ cells by removing $CD4^+$ cells and positively selecting $CD8^+$ cells. This preparation was 97–98% $CD8^+$ in repeated experiments. Percentages of $CD4^+$ and $CD8^+$ T cells in the spleen after FV inoculation were determined by flow cytometry in $CB6F_1$ mice immunized with peptide i. To reconstitute the full number of T cells that belonged to each subset in the immunized mice, unimmunized recipient mice were injected intravenously with 2×10^7 to 2.5×10^7 $CD4^+$ or $CD8^+$ T cells per mouse.

Depletion of $CD4^+$ T cells

Anti-mouse CD4 mAbs were purified from culture supernatant of the hybridoma cell GK 1.5 (29) as described previously (13, 25). Control rat myeloma IgG was purchased from Zymed Laboratories, Inc. The amount of the mAbs required for complete depletion of $CD4^+$ T cells from $CB6F_1$ mice was determined by intravenously administering the purified mAb and monitoring the number of $CD4^+$ and $CD8^+$ cells in the spleen by flow cytometry. The schedule of mAb administration finally adopted was as follows: $CB6F_1$ mice were immunized with 3 μg per mouse of peptide i emulsified in CFA. Three weeks later, mice were intravenously given 125 μg per mouse purified anti-CD4 mAb. Five additional intravenous doses of 125 μg per mouse anti-CD4 mAb were given 2, 4, 6, 9 and 18 days after the first administration. The negative-control rat IgG was given to a separate group of mice on the same schedule. Mice were inoculated with 150 spleen focus-forming units (SFFU) FV 7 days after the beginning of the mAb administration. Peripheral blood was collected from three representative animals at each time point through the tail vein at post-infection day (PID) 3, 6, 10 and 13, and flow cytometric analyses were performed to confirm the absence of $CD4^+$ T cells.

Statistical analyses

Differences in survival curves expressed by the Kaplan–Meier method were compared by a Mantel–Haenszel logrank test using GraphPad Prism 3 (GraphPad Software, Inc., San Diego, CA, USA). The numbers of mice that developed or lacked splenomegaly were compared between the immunized and unimmunized groups by Fisher's exact test. Average numbers of infectious centers between experimental groups and anti-leukemia cell antibody titers were compared by Mann–Whitney's *U*-test because these values were not expected to follow a Gaussian distribution. Differences in IgM and IgG titers of virus-neutralizing antibodies were compared by paired *t*-test. Spleen weights and percentages of $TER\text{-}119^+$, $gp70^+$ cells in the spleen and bone marrow between the immunized and unimmunized groups of mice were compared by Student's or Welch's *t*-test depending on whether the variances of the compared samples were estimated to be equal or not.

Results

Suppression of the early growth of FV-infected erythroid cells and prevention of leukemic death in highly susceptible $CB6F_1$ mice by immunization with a single-epitope $CD4^+$ T cell vaccine

Mice of BALB/c background are extremely susceptible to FV-induced disease, and $CB6F_1$ mice all died within 60 days after infection with only 15 SFFU of FV without showing any signs of spontaneous recovery (Fig. 1a). This was striking because even (B10.A × A/WySn)F_1 mice that have been used as a strain typically susceptible to FV infection have shown mortality rates of 70–80% at 90–100 days after inoculation with 15 SFFU FV (1, 5). Therefore, the following immune protection experiments were performed in $CB6F_1$ mice with 150 SFFU of FV to ensure that peptide-induced immune responses protect this highly susceptible strain of mice from doses of FV large enough to kill all unimmunized animals.

The efficacy of peptide i in priming $CD4^+$ T cells *in vivo* has been demonstrated by the establishment of $CD4^+$ T cell clones reactive to this peptide from the peptide-immunized $CB6F_1$ mice (23), and by more pronounced expansion of $CD4^+$ T cells in the spleen after FV challenge in the peptide-immunized than in the unimmunized control $CB6F_1$ mice (14). To directly demonstrate the priming of $CD4^+$ T cells in peptide-immunized